



Contents lists available at ScienceDirect

International Journal of Hydrogen Energy

journal homepage: www.elsevier.com/locate/he

The next generation of low tritium hydrogen isotope separation technologies for future fusion power plants

Lawrence Shere^a, Alfred K. Hill^{a,*}, Timothy J. Mays^a, Rachel Lawless^b, Rosemary Brown^b, Semali P. Perera^a

^a Department of Chemical Engineering, University of Bath, Bath, BA2 7AY, UK

^b Culham Science Centre, Abingdon, OX14 3DB, UK

ARTICLE INFO

Handling editor Suleyman I. Allakhverdiev

Keywords:

Hydrogen isotope separation
Cryogenic distillation
Adsorption
Palladium
Fusion energy
Hydrogen membranes

ABSTRACT

The separation of hydrogen isotopes is a vital step in preparing tritium and deuterium fuels for future fusion power plants. This represents a fundamental challenge to fusion energy since the separation process must be able to handle high throughputs of hydrogen isotopes whilst maintaining a low tritium inventory, because tritium is highly radioactive. There are many possible isotope separation techniques, however none that are currently deployable can meet the demands required. To address this gap, recent developments have improved existing processes and created new high-performance processes including Thermal Cycling Absorption Process (TCAP), electrochemical graphene sieving and absorptive separation based on quantum sieving. In this article, ten of the most promising future hydrogen isotope separation technologies are reviewed, to understand the development route to a process that addresses this key challenge of fusion energy.

1. Introduction

1.1. Background

Global energy demand is predicted to increase by 40 % from 2019 to 2040 due to rapid population growth and urbanisation [1]. The Paris Agreement of 2015 set out the goal of keeping global temperature rise this century to below 2 °C above pre-industrial levels, and to pursue efforts to limit the temperature rise to 1.5 °C [2]. These ambitious goals will require simultaneous rapid decarbonisation and expansion of energy generation [1]. One possible source of future energy is nuclear fusion but it faces several technical challenges; one of these is the need for a large scale, energy efficient hydrogen isotope separation system. Fusion reactors are expected to burn-up only about 2 % of the mixed deuterium and tritium fuel, and so recycling of the exhaust gases is an important step for efficient operation [3,4].

The main requirements of the isotope separation system for future fusion plants are low tritium inventory, high separation and energy efficiencies. These are essential considering that isotope separation will need to be scaled-up to process much larger throughputs (see section 1.3). Tritium, ³H, is the heaviest isotope of hydrogen and is highly radioactive. Due to the radiation hazard from tritium both onsite and to

the local environment, strict inventory limitations are placed on tritium handling processes [5]. Reduced tritium inventories can be achieved by improved process kinetics, which reduces the tritium residence time. Isotope separation efficiency is another important requirement since the similar properties of hydrogen isotopes makes them difficult to separate, requiring impractically large and inefficient separation plants. Energy efficiency is also important since future fusion plants will need to demonstrate net electrical energy generation, meaning energy consumption cannot be excessive. Unfortunately, there is no currently available isotope separation process that can satisfy these three main requirements. This has led to a renewed research interest in developing alternative isotope separation methods for future fusion plants (see Fig. 1).

An important metric of selectivity for a process is the separation factor, α . When comparing different processes, it is important to take into account the different hydrogen isotopologues (e.g., H₂, HD, D₂, DT, T₂, HT). For example, H₂/HD and H₂/D₂ mixtures have the same atomic isotope composition but the separation factor is much lower for H₂/HD. Cryogenic distillation (CD) is currently the leading conventional hydrogen isotope separation technique. CD separation is based on the slightly different volatility of hydrogen isotopes which leads to a reasonably low separation factor of 2.3 for H₂/D₂ or 1.5 for H₂/HD at 24 K [6]. CD has a high complexity and energy intensity due to the extreme

* Corresponding author.

E-mail address: A.K.Hill@bath.ac.uk (A.K. Hill).

<https://doi.org/10.1016/j.ijhydene.2023.10.282>

Received 11 August 2023; Received in revised form 12 October 2023; Accepted 27 October 2023

0360-3199/© 2023 The Authors. Published by Elsevier Ltd on behalf of Hydrogen Energy Publications LLC. This is an open access article under the CC BY license (<http://creativecommons.org/licenses/by/4.0/>).

Acronyms

AVLIS	Atomic Vapour Laser Isotope Separation
CAQS	Chemical Affinity Quantum Sieving
CD	Cryogenic Distillation
CECE	Combined Electrolysis Chemical Exchange
GC	Gas Chromatography
GS	Girdler Sulphide
HETP	Height Equivalent to Theoretical Plate
MLIS	Molecular Laser Isotope Separation
MOF	Metal Organic Framework
PSA	Pressure-Swing Adsorption
QS	Quantum Sieving
TCAP	Thermal Cycling Absorption Process
TSA	Temperature-Swing Adsorption
VPSA	Vacuum Pressure-Swing Adsorption

temperatures required and high tritium inventory due to the liquid hydrogen phase.

This article will critically review developments of ten hydrogen isotope separation technologies for potential application in future fusion plants and provide quantitative data such as separation factor. Some hydrogen isotope technologies are inherently unsuitable for separation of highly tritium enriched mixtures (chemical exchange processes, gas centrifuge, electrolysis) and details of these can be found in the appendix (refer to [supplementary information A1 - A4](#)). In the first part of the article, sorption-based techniques are reviewed including Adsorption (based on quantum sieving), Gas Chromatography and TCAP. In the next sections, membrane separation based on metallic (palladium alloys), non-metallic and novel graphene membranes are compared. Cryogenic distillation is then discussed, which will be important technology for the future ITER project as it is currently the only readily deployable technology at this scale. In the final sections, alternative processes including Plasma-Chemical separation, Thermal diffusion and Laser isotope separation are reviewed. This article will be the first time many these technologies have been reviewed in the literature, providing a timely discussion for their application in future fusion projects.

1.2. The challenge of tritium

Tritium is difficult to contain, since it can easily diffuse through solids, such as metals, and can exchange with hydrogen compounds to form tritiated water (HTO, DTO, and T₂O). Tritiated water is a significant radiation hazard to human health, since it is readily absorbed into the body and has a long biological half-life of approximately 10 days [5]. Tritium handling processes require special considerations, with multiple layers of containment. A greater risk is a fire scenario, which has the combined hazard of the flammable hydrogen isotopes, and the uncontrolled release of oxidised radioactive tritium into the local atmosphere [5]. The hazard from leaks and fire increases proportionally with the size of tritium inventory onsite [3].

Water and other liquid phase hydrogen compounds contain more hydrogen atoms per litre than gaseous hydrogen and even liquid hydrogen as shown in [Table 1](#). This enables water-based separation processes to have greater throughputs than gaseous hydrogen processes, but the tritium inventory is generally higher. As it can be seen, tritium decay also releases significant heating power which may need to be accounted for in process energy balances, especially for Cryogenic Distillation.

1.3. Isotope separation requirements of future fusion plants

Isotope separation is required to rebalance the ratio of tritium to

Table 1

–Volume-based properties of tritium (T₂) and tritium compounds calculated in this paper from density (kg m⁻³) values and tritium radiation data.

	Gaseous nT ₂ (288 K, 1 bar)	T ₂ O (288 K)	Liquid nT ₂ (22 K)	Hydride (PdT _{0.60})
Equivalent tritium molar density, mmol T ₂ cm ⁻³	0.0416 [7], ^a	55.2 [8]	44.5 [9]	30.3 [10]
Radiation, GBq cm ⁻³ (100 % tritiated feed)	0.089	118.3	95.56	65.07
Decay heat, mW cm ⁻³ (100 % tritiated feed)	0.08087	107.2	86.59	58.96

For the isotope rebalancing step, gaseous hydrogen feeds are preferred since the feed is already in this form and the tritium inventory of gaseous hydrogen processes is generally low. Processes with hydrogen compound feeds are generally used in applications where tritium inventory is less of a concern, such as heavy water separation and the initial stages of tritium removal from water.

^a Based on D₂ molar density value, 1.944 W mol T₂⁻¹ [11,12], 1 Ci = ~37 GBq, 9616.3 Ci g T₂⁻¹ [8].

deuterium in the exhaust and remove protium (¹H), an undesired contaminant introduced from outgassing and permeation through the pipework. The Protium Removal step is required to keep the protium concentration below 1 %, as a current working estimate [13]. Once the DT fuel is prepared it is injected into the fusion reactor. Currently the favoured fuelling method is pellet injection in which solid fuel pellets are injected at very high speeds (~300 m s⁻¹). Only a small portion of the injected fuel is expected to reach the plasma core, and some will escape the magnetically confined plasma core before fusion can occur [14]. This explains the low expected burn-up rate of ~2 %. This plasma exhaust is then recycled back to the inner fuel loop.

The throughput of tritium will be much higher than previous projects. The DEMO power plant, for example, is a conceptual plant, expected to consume approximately 313 g of tritium per day to produce 2 GW of energy, compared to ITER, which will only produce 0.4 g of tritium per day [3,15]. Due to the expected low burn-up rate in the fusion reactor, the inner fuel cycle is designed to recycle the exhaust gases. The tritium throughputs in the inner fuel loop will be much higher than the amount of tritium consumed by the reactor. Assuming 313 g of tritium is consumed in a day and a burn-up ratio of 2 %, the required tritium throughput of tritium in the inner loop could be as high as 13 kg day⁻¹ (~5200 mols day⁻¹) which is roughly 1000 times that of ITER. For DEMO, some of the exhaust gases can bypass the isotope separation system [16]. Unlike ITER, DEMO will require a mixed 50:50 deuterium and tritium for the reactor and so high isotopic purity is not a key requirement which widens the potential technology choices [3,16].

2. Adsorption (PSA/VPSA/TSA processes)

Microporous adsorbents such as zeolites and metal-organic frameworks (MOFs) have been shown to have a higher affinity for adsorbing heavy hydrogen isotopes at cryogenic temperatures due to an effect known as Quantum Sieving (QS). Hydrogen isotope molecules have almost identical molecular hard-core size (0.24 × 0.24 × 0.314 nm [17]) but the differences in molecular mass can lead to different quantum contributions when confined in the pores of adsorbents. QS was first proposed for isotope separation by Beenakker et al. [17] who noted that when the pore is of similar size to the molecule, the gap between the pore wall and the hard core of the guest molecule can become very small (see [Fig. 2](#)). For light molecules, such as hydrogen isotopes, the gap size can approach the thermal de Broglie wavelength at low temperatures. Under these conditions, the molecule's energy levels become quantised, and quantum effects such as Zero-Point Energy (ZPE) have a greater influence on adsorption. The ZPE acts as a repulsive force which inhibits adsorption. Due to their higher mass, heavier isotopes have lower ZPE and smaller corresponding de Broglie wavelength. By selecting a

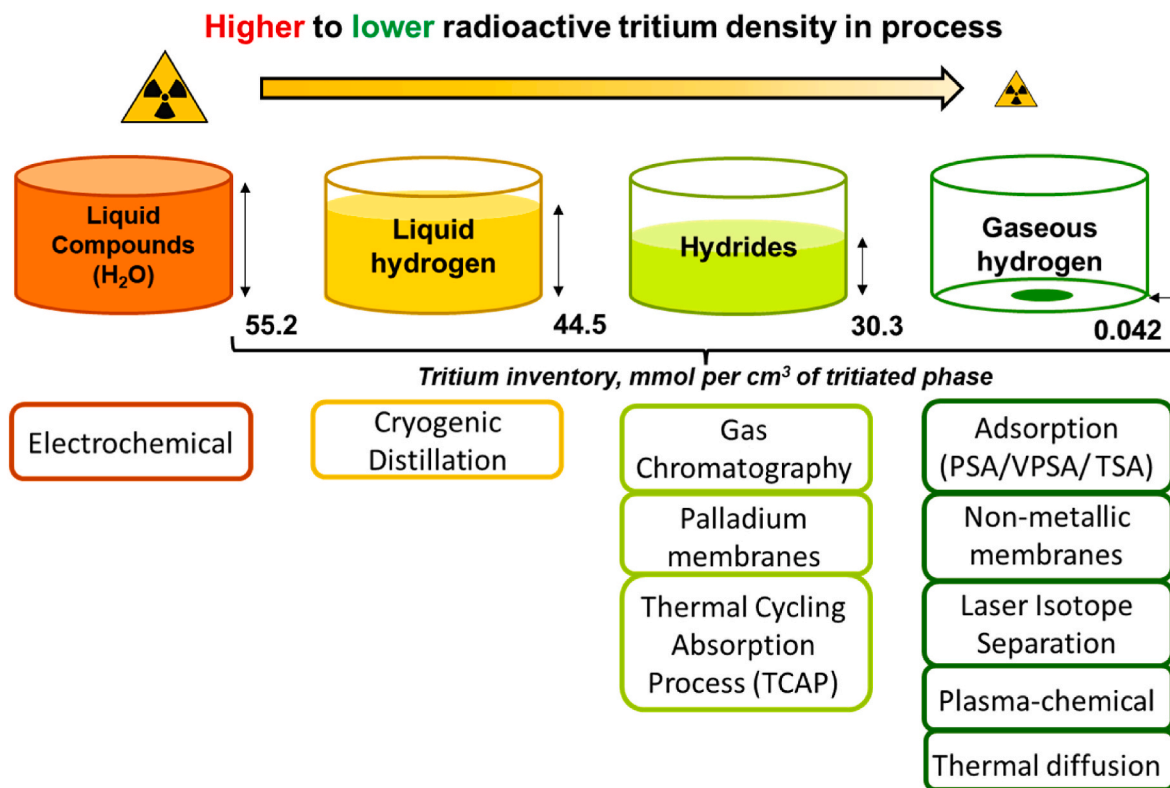


Fig. 1. Hydrogen isotope separation technologies reviewed in this article categorised by the main phase of hydrogen used.

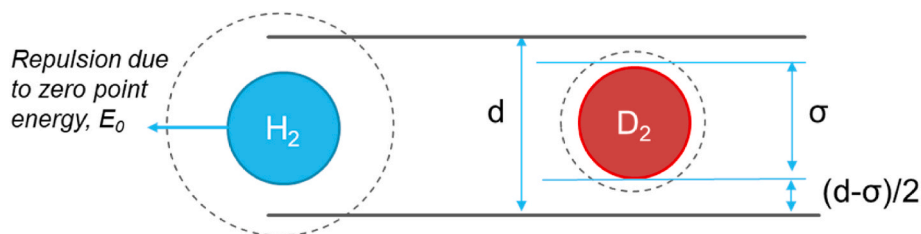


Fig. 2. Quantum sieving effect - hydrogen molecules are confined in narrow pores, the gap size $(d-\sigma)/2$ can approach the de Broglie wavelength and the zero-point energy becomes significant.

suitable pore size, lighter isotopes will be repelled but heavier isotopes are still able to adsorb. The QS mechanism can affect both equilibrium and the kinetics of molecular transport in the pores.

In the last two decades, quantum sieving has been tested experimentally on many different types of adsorbents and has been shown to be effective for separating hydrogen isotopes. As shown in Fig. 3, some adsorbents have been reported to have higher isotope selectivity and uptake than conventional high-performance materials such as palladium which is used in Gas Chromatography. However, these adsorbents require cryogenic operating temperatures (<77 K) with many of the highest performing adsorbents shown in Fig. 3 requiring even lower temperatures of 25–48 K. Compared to room temperature processes this will have increased operating costs and complexity of operation especially during start-up. Table 2 provides further details for adsorbents tested from a wide range of experimental studies.

Of all the adsorbents tested in the last ten years, Metal-Organic Frameworks (MOFs) have been the most widely investigated for hydrogen isotope separation and have some of the highest reported isotope selectivity values. MOFs are crystalline materials composed of metallic nodes connected by inorganic ligands which can form a porous infinite lattice structure. The pore size of MOFs can be tailored to enhance the quantum sieving effect. Oh et al. measured the selectivity of

MOFs with 4 different pore sizes at temperatures below 77 K, and found an optimal pore size of approximately 3.4 Å [37]. Mondal et al. [33] found that selectivity could be enhanced in the IFP framework from ~1.69 to 2.41 by reducing the pore size from 4.2 to 3.1 Å. Kim et al. investigated MIL-53, a MOF which can undergo a transition between narrow pore (2.6 Å) and large pore configurations (8.5 Å). In the transition regime, an optimal pore size could be made and high selectivity of 10.5 could be achieved at 40 K [43].

MOFs can contain open metal sites with high heats of adsorption for hydrogen (6–33 kJ/mol) which show high isotope selectivity through an effect termed Chemical Affinity Quantum Sieving (CAQS) [44]. This was first demonstrated in MOF-74 which is a MOF framework that can be synthesised with a variety of different transition metals (Mn, Zn, Mg, Fe, Co and Ni). It was found that higher affinity metal sites (Ni and Co) exhibited very high selectivity compared to lower affinity metals (Fe, Mn) [45]. Cu(I) open metal sites as in Cu(I)-MFU-4l have been reported to have one of the highest adsorption enthalpies for hydrogen (32 kJ/mol) [46] leading to high D₂/H₂ selectivity of 11 at relatively high temperatures (100 K). The H₂ adsorption enthalpy for Cu(I) is comparable in magnitude to H₂ sorption enthalpy of palladium (38–39 kJ/mol) [10,47]. This high heat of sorption makes it difficult to remove the adsorbed hydrogen isotopes from the adsorbent. Furthermore, open

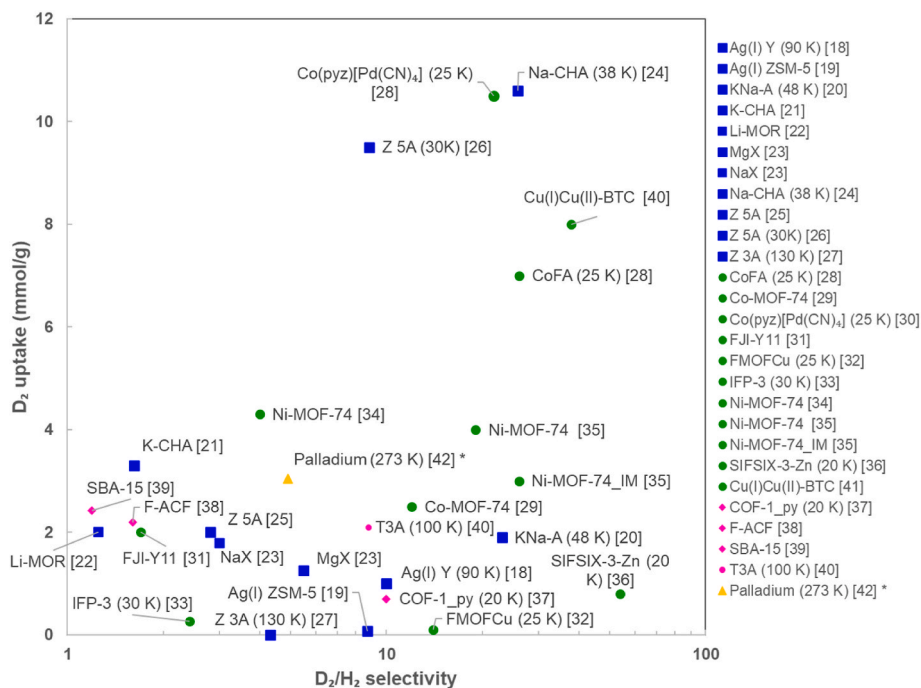


Fig. 3. –Adsorbents tested for hydrogen isotope separation showing selectivity and uptake compared to palladium* used in conventional isotope separation. Material types: Metal-Organic Frameworks (MOFs) (green circles), Zeolites (blue squares) and other adsorbent types (purple circles). Unless stated otherwise, materials have been tested at 77 K. * Palladium – for purpose of comparison to adsorbents, separation factor value of H_2/D_2 is inverse and derived as the product of H_2/HD and HD/D_2 . (For interpretation of the references to colour in this figure legend, the reader is referred to the Web version of this article.)

metal sites generally have poor chemical stability. Unfortunately, due to their organic components, MOFs are likely to degrade in tritium irradiated environments and so may be inherently unsuitable.

Another class of adsorbent are zeolites, which are crystalline aluminosilicate materials that have been widely tested for hydrogen isotope separation. Zeolites have been proven for long term use in tritium environments for capturing tritiated water [48]. They have very uniform pore sizes which can be tuned to the optimal size by selecting the suitable zeolite type. The effective pore size of Zeolite A can be made to be 3, 4 or 5 Å by changing the extra-framework cations. It was reported that by reducing the pore size of zeolite A from 5 Å to 4 Å, the selectivity was enhanced at 77 K and 1 kPa from 2.8 to ~3.4 [49]. Chabazite (CHA) zeolite containing large caesium cations has been reported to show a discriminative effect between H_2 and D_2 near 293 K due to a novel trapdoor effect [50], although adsorption uptake data was not provided. Bezverkhyy et al. [24] recently reported a very high selectivity of 25.8 for chabazite zeolite at 38 K. It was found that very long equilibration times were needed (24 h) to achieve high selectivity. Zeolites generally have a lower heat of adsorption for H_2 (4–6 kJ/mol) but can be modified to contain metal sites such as Cu(I) and Ag(I) leading to high selectivity through the CAQS effect [18,19,51].

For practical large-scale separation of hydrogen isotopes, adsorbents are used in filled columns and undergo a cycle which enables the adsorbent to be regenerated to recover the adsorbed gases. Regeneration, which involves desorbing the gas from the adsorbent to make it ready for the next adsorption cycle, can be done by raising the temperature of the column as in Temperature Swing Adsorption (TSA). This can be a slow process especially in large columns, reducing the time available to utilise the bed for adsorption. For large scale separation of high throughput gases, Pressure-Swing Adsorption (PSA) is the preferred option. PSA regenerates the packing by a reduction in gas pressure which is not limited by heat transfer and so can be completed very quickly providing much better bed utilisation time for adsorption. If below atmospheric pressures are used it is known as Vacuum Pressure-Swing Adsorption (VPSA). Common cycle times for PSA can vary from

around 15 min [52,53] down to the order of seconds [52]. Normally more than one adsorption column is used to provide constant flow and better recovery of the pressurisation energy and product gas. PSA is efficient for adsorbents with low heat of adsorption and so MOFs and zeolites containing open metal sites may not work well for PSA. The fast cycle times and efficient bed utilisation time of PSA will reduce the required column volume and so PSA will tend to have significantly lower tritium inventory than TSA.

Kotoh et al. tested 13X and 5A zeolite spherical pellets at 77 K using PSA operation between 1 bar and vacuum pressure to successively enrich D_2 in H_2 [54,55]. An enrichment factor of 1.3–1.4 was measured for zeolite 13X. Separation performance was lower than predicted from the isotherm data partly due to the D_2 concentration distribution that forms in the bed and incomplete desorption by depressurisation alone [55,56]. Temperature assisted evacuation removed the residual D_2 and this led to high D_2 enrichment as high as 9.21 for 13X [56]. The use of a temperature assisted evacuation in the last cycle led to much higher enrichment than with the pressure change alone, and so the authors suggest incorporating temperature-swing to further increase efficiency [55]. This combination was demonstrated in a recent paper to be effective for hydrogen isotope separation [57]. Using a two-column arrangement with a cyclic operation in which the D_2 concentration was enriched from 3.9 % to above 95 % after 6 cycles. The cycle time was 39 min with a combined enrichment factor of 19.7.

A PSA process separation of hydrogen isotopes has been demonstrated using zeolites at liquid nitrogen temperatures (77 K) and vanadium hydride [58]. Fitzgerald et al. [59] analysed the effect of the adsorbent-adsorbate binding energy on the recovery ratio and enrichment factor from TSA. MOFs such as Cu(I)MFU-1 and MOF-74 have high binding energy which tends to lead to high separation factors and higher operating temperatures. However due to the overlap of the H_2 and D_2 desorption peaks with temperature, it is not possible to recover all the D_2 at high purity. Fitzgerald et al. predicted that the fraction of D_2 recovered initially increases with binding energy but tends to plateau at about 5–10 kJ/mol. It was reported that adsorbents with a sharp desorption

Table 2

Adsorbents tested for hydrogen isotope separation, including experimental apparatus used (Mt-Ads = Multi-gas, Sg-Ads = single gas adsorption, IAST = Ideal Adsorbed Theory).

Mat name	Mat Type	Accessible Pore Size (Å)	Apparatus	Temp (K)	Pressure (kPa)	D2 capacity (mmol/g)	Sel(H ₂ /D ₂)	Ref.
3A	Zeolite	3	Isobars (Co-Ads)	130, 140 & 160	8.5	0.001, 0.003, 0.012	4.33, 3.04 & 2.32	[27]
13X, 5A	Zeolite	8, 5 *	Isotherms (Co-Ads)	77	1	2.0, 1.8	2.8, 2.5	[25]
Ag(I) Y	Zeolite	8*	TDS	20, 77, 90	1	16.5, 2, 1	1, 5.5, 10	[18]
Ag(I) ZSM-5	Zeolite	5.4–5.6 *	TDS	77 & 160	1	0.08, 0.009	8.7 & 3.1	[19]
Cu-ZSM-5	Zeolite	5.4–5.6 *	TDS	100, 200, 273	0.001	n.c.	24.9, 5.4, 1.2	[51]
5A	Zeolite	5.82	TDS	30, 40, 60	5	9.5, 8.5, 5.5	8.83, 4.98, 4.04	[26]
MgX, NaX	Zeolite	8 *	Isotherms (Co-Ads)	77	~10	1.26, 1.79	5.5, 3	[23]
Na-CHA	Zeolite	3.8	Isotherms (Co-Ads)	38, 51, 77	65	10.6, n.g., n.g.	25.8, 8, 3	[24]
Ca-CHA	"	3.8	"	39, 52, 77	65	12.9, n.g., n.g.	18.3, 6, 3	[24]
Na-CHA	Zeolite	3.8	Isotherms (Co-Ads)	40, 58	65	n.g.	13, 3.75	[60]
NaK-CHA	"	3.8	"	40, 58, 77	65	n.g.	10, 3.75, 2.5	[60]
Li-CHA	"	3.8	"	40, 54, 77	65	n.g.	10.5, 4, 2.5	[60]
NaA	Zeolite	4	Isotherms (Co-Ads)	48, 57, 77	65	10.3, 9.4, 12	8.5, 5, 2.9	[20]
KNaA	"	3–4	"	48, 57, 77	65	1.9, 5.3, 10	23, 5, 5.5	[20]
Li-MOR	Zeolite	8	Isotherms (Idv-Ads)	77, 195	1	2, 4E-3	1.25, 1.1	[22]
Ca-MOR	"	8	"	77, 195	1	2, 0.01	1.25, 1.7	[22]
5A, 10X, Y	Zeolite	5, 8, 7	Breakthrough (Co-Ads)	77	31	4.3, 3.41, 3.83	1.51, 1.45, 1.31	[39]
SBA-15	Mesoporous silica	51	"	"	"	2.42	1.19	[39]
K-CHA	Zeolite	3.4	Isotherms (Idv-Ads)	77, 201, 250	10	3.3, 15.5, 8.3	1.62, 1.02, 1.00	[21]
Na-CHA	"	3.4	"	"	"	1.45, 12.33, 5.90	2.23, 1.11, 0.83	[21]
ACF	Activated carbon	~0.7	Isotherms (IAST)	77	93	7.8	1.4	[38]
F-ACF	"	~0.7	"	"	"	2.2	1.6	[38]
SIFSIX-3-Zn	MOF	3.86	TDS	20, 25	25	0.8, 0.4	54, 40	[36]
CoFA	MOF	4	TDS	25	100	7	26	[28]
Cu(I)-MFU-4l	MOF	n.g.	TDS	90, 100	1	n.g.	7.1, 11.1	[46]
Fe-MOF-74	MOF	n.g.	Isotherms (IAST)	77, 87, 120	1	4, 2, 0.1	2.5, 2.2, 1.5	[34]
Co-MOF-74	"	n.g.	"	77, 87, 120	1	5.5, 4.8, 0.3	3.2, 2.6, 1.7	[34]
Ni-MOF-74	"	n.g.	"	77, 87, 120	1	4.3, 3.9, 0.5	4.0, 3.3, 1.9	[34]
Ni-MOF-74	MOF	11	TDS	25, 60, 77	1	17, 6, 4	7, 16, 19	[35]
Ni-MOF-74-IM	"	n.g.	"	"	"	14, 5, 3	6, 20, 26	[35]
MIL-53(Al)	MOF	2.6–8.5	TDS	40	1	2.9	13.6	[43]
Co-MOF-74	MOF	11	TDS	20, 60, 80	3	12, 2.5, 1	3, 12, 6	[29]
Cu(I)Cu(II)-BTC	MOF	6.2, 8.7, 11.0	TDS	30	1	8	37.9	[41]
DUT-8(Ni)	MOF	n.g.	TDS	23.3	10, 70	0, 40	11.6	[61]
FJI-Y11	MOF	3.8	Isotherms (IAST)	77, 87	1, 100	77 K 2.0, 8.9 87 K 1.3, 7.6	77 K 1.7, 1.8 87 K 1.5, 1.5	[31]
HKUST-1	MOF	10.7	"	"	1, 100	n.g.	77 K 1.5, 1.4 87 K 1.4, 1.4	[31]
Ni ₂ Cl ₂ BBTA	MOF	n.g.	Co-Ads	77, 87	1	1.7, 1.0	4.5, 4.0	[62]
IFP-1, IFP-3	MOF	4.2; 3.1	TDS	30	1	0.71, 0.27	1.69, 2.41	[33]
IFP-7, IFP-4	"	2.1, 1.7	"	77	"	0.16, 0.20	1.10, 1.97	[33]
MFU-4	MOF	2.52	TDS	40, 60, 70	1	n.c.	6.9, 7.5, 2.8	[63]
COF-1 _{Py}	COF	n.g.	TDS	20, 40, 70	2.6	0.7, 0.75, 0.15	10, 5.5, 3	[64]
Co(py ₂ z)[Pd(CN) ₄]	MOF	3.9	TDS	25, 40, 60	1	10.5, 7.5, ~1.5	21.7, 5, 2	[30]
FMOFCu	MOF	2.5–3.6	TDS	25, 40, 87	1	0.1, 0.37, 0.05	14, 6, 2	[32]
2β	MOC	<3	TDS	30, 77, 100	20	0.16, 1.1, 0.21	8.5, 2, 1.7	[65]
T3A	Carbon (CMS)	3	TDS	100, 150	60	2.1, n.g.	8.8, 3.7	[40]

profile and large differences in the H₂/D₂ binding energy would be able to achieve both high enrichment factors and recovery ratios [59].

In summary, many adsorbents including zeolites and MOFs have been reported to have very high selectivity for hydrogen isotopes through quantum sieving. A great deal of progress continues to be made in understanding how different pore types, high affinity adsorption sites and novel breathing transition mechanisms can all be used for isotope separation. However, these adsorbents currently require cryogenic temperatures, and have practical issues such as low hydrogen uptake, poor stability in tritium radiation environments and difficulty desorbing the hydrogen isotopes. PSA has been demonstrated for hydrogen isotope separation but with a lower separation factor than was predicted from the equilibrium adsorption isotherms due to adsorption kinetic limitations. Higher enrichment and product recovery could be achieved with an additional thermal desorption/vacuum step after depressurisation. Future work should investigate PSA parameters and selecting adsorbents that can achieve good separation performance with no or minimised

need for a thermal desorption step.

3. Gas chromatography

Gas Chromatography (GC) separates gas mixtures based on the different strengths of adsorption/absorption to a stationary bed of solid sorbent (most commonly palladium) held within a column in a batch cycle. Unlike other adsorbent processes, chromatography uses a carrier gas to push the gas components through the column. The carrier gas can be an inert gas such as He or Ne as in elution chromatography or a pure active gas component such as H₂ as in displacement chromatography (see Fig. 4). Chromatography achieves a high separation efficiency compared to other adsorbent processes [52], but the carrier gas increases the complexity of operation, and reduces the availability of the column for sorption.

Palladium (Pd) metal is the most common sorbent used for preparative hydrogen isotope separation due to its high separation efficiency

and large hydrogen capacity at room temperature. Pd preferentially absorbs lighter hydrogen isotopes with a reasonable separation factor of $\alpha_{HD} = \sim 2$ at 293 K [66]. Pd also acts as a catalyst for heteromolecular conversion and inter-fractions of DT, HT and HD are obtained. To maximise the available Pd and improve separation performance, highly porous media such as sponge Pd [67], Pd-Al₂O₃ [68–70] or Pd-kieselguhr [71] are used. Du et al. [72] prepared nanoporous palladium with 5 nm pores which enabled faster absorption and higher selectivity at low temperatures. Alloys of Pd with 5 wt% Pt can have improved separation properties and lower heat from hydride formation [73].

The major drawback of Pd is its high cost. The price of Pd has significantly increased in recent years from approximately 25,000 USD per kilo in 2015 to 44,000 USD per kilo in 2023 [74]. The Active Gas Handling System at JET, for example, contains 1.57 kg of Pd [75,76]. Cheaper alternative metal hydrides such as Vanadium (V) or LaNi₅ have been tested but the separation performance is generally lower and can require cryogenic operating temperatures (see Table 3) [77]. Physical adsorbents such as Al₂O₃ and zeolites have been demonstrated for preparative GC but generally find more use in analytical hydrogen isotope GC [78–82] and equilibrium absorption separation [83]. A novel adaptation to the GC process using a temperature programmed column was developed by Ontario Hydro Technologies [84]. By maintaining a temperature gradient, the throughput and separation factor were improved using molecular sieve 5A packing and helium carrier gas [84]. This concept may enable the use of cheaper molecular sieves by enhancing their performance.

Pd packings for isotope separation were first developed in the 1950s [71] with one of the first reports in 1956 by Glueckauf & Kitt who used Pd black supported on asbestos as the column packing [90]. Batch operated Pd GC has become a well-established technique, which has been used at CEA/Valduc for tritium gas production [69] and as part of the Active Gas Handling System (AGHS) at JET. In both of these systems, GC was used to produce high purity tritium, but was found to be unsuitable for detritiation purposes [69,75,102]. GC for preparatory hydrogen isotope separation is most commonly operated in displacement mode (see Fig. 4), when using Pd packing. During the displacement cycle, the Pd contains high hydrogen concentrations which improves the separation factor [66,103]. At the end of the cycle, protium must be removed from the packing by heating from room temperature to around 473 K in flowing helium gas [102]. The time required to heat and regenerate the column greatly reduces the column utilisation time for isotope separation, especially at larger scale. Multiple GC columns can be operated to achieve semi-continuous operation with increased recovery by recycling of inter-fractions [104]. Other chromatography modes have been tested such as self-displacement [105], frontal [105] and frontal displacement [68] but the isotope recovery is far less than the typical hydrogen-displacement process [105].

Pd is favoured for GC because it combines three important characteristics: high separation factor ($\alpha_{H/D} = \sim 2$) [85], large hydrogen capacity at room temperature (up to ~ 70 % atoms in PdH_x can be hydrogen [106]) and fast kinetics [77,85]. Pd has a selectivity for light isotopes (protium) whereas many other metal hydrides demonstrate the inverse selectivity. This is explained by the existence of two opposite isotope selectivity effects [10]. The first effect is due to the higher heat of hydride formation for protium than heavier hydrogen isotopes [106]. This effect is strongest in Pd due to the high affinity for hydrogen and causes its selectivity for protium. The second effect is the instability in the metal lattice caused by hydrogen atoms [107,108]. Protium has the greatest destabilising effect which leads to preferential selectivity for heavier isotopes. This is the dominant effect in some alternative metal hydride systems, notably Vanadium and LaNi₅ [87]. The interplay of the two effects described can lead to either an overall normal or an inverse isotope effect in metal hydrides at a given temperature [108]. The lattice parameter of Pd can be altered by alloying with other metals such as Cu, Ag and Au. In particular, Pd_{0.9}Cu_{0.1} has a similar separation factor to

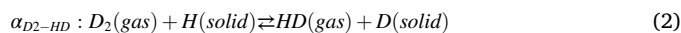
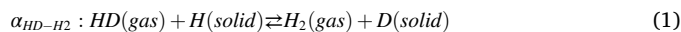
Table 3

Comparison of the most promising metal hydrides and adsorbates for Gas Chromatography.

Material	Advantages	Disadvantages
Palladium (Pd) [66,85]	<ul style="list-style-type: none"> • High separation factor ($\alpha_{HD} = \sim 2$ at 293 K [85]). • High hydrogen uptake • Very fast isotope exchange rate at room temperature. • Easy to work with – Insensitive to gas impurities and oxide layer removed in hydrogen environments (at temperature of >300 K) [10]. 	<ul style="list-style-type: none"> • High material cost. • Large temperature swing required from close to ambient (298 K) to a minimum desorption temperature of 433 K
Vanadium (V) [86–90]	<ul style="list-style-type: none"> • Strong inverse equilibrium isotope separation (roughly $1/\alpha_{HD} = 1.7 \pm 0.3$ at room temperature measured from Ref. [87] and similar value to ratio of H/D vapour pressures in Ref. [89]). • Beneficial catalytic effect from metal impurities in commercial vanadium. May be possible to enhance performance using metal dopants [86,87]. 	<ul style="list-style-type: none"> • Isotope exchange rate is very slow at room temperature [90]. • Highly sensitive to gas impurities such as oxygen [86]
LaNi ₅ and related compounds [77,91,92]	<ul style="list-style-type: none"> • Fast isotopic exchange rate at room temperature (HETP of 1.5 cm at 473 K [91]. • Ni atoms can be substituted for other metals such as Al, Cr, Cu enabling alteration of the alloy properties [93]. 	<ul style="list-style-type: none"> • Low inverse separation factor (LaNi_{4.7}Al_{0.3} at room temperature, $1/\alpha_{HD} = \sim 1.25$ [85]) • Optimised separation efficiency of LaNi₅ may require “dry ice” temperatures (195 K) [77].
Zr based alloys [77,90,94]	<ul style="list-style-type: none"> • High hydrogen adsorption capacity such as ZrCoH_{1.8} [95] 	<ul style="list-style-type: none"> • Optimal operation at “dry ice” temperatures (195 K) [77] • Small separation factor (ZrNiH₃ – $\alpha_{HT} = 1.05$ [90])
Mg ₂ Ni [96]	<ul style="list-style-type: none"> • Addition of Ni or Cu reduces activation temperature of MgH₂ as low as 473 K [93]. 	<ul style="list-style-type: none"> • High temperatures required to improve kinetics (HETP_{min} = 3.5 cm reported at 573 K for a Mg₂Ni particle bed) [96] • Separation factor not reported [96]
Al ₂ O ₃ and zeolites [83,97,98]	<ul style="list-style-type: none"> • Much cheaper than other materials. 	<ul style="list-style-type: none"> • Requires cryogenic temperatures such as 77 K. • Separate HD, HT and DT peaks are produced reducing separation performance.
Uranium [99, 100]	<ul style="list-style-type: none"> • Very high hydrogen absorption capacity [100] (On atom basis, 75 % of uranium hydride is hydrogen [101]). • Fast adsorption kinetics possible, theoretical minimal HETP of 0.72 mm [100]. 	<ul style="list-style-type: none"> • High dissociation temperature (473 – 673 K) • Separation factor (at equilibrium $\alpha_{HD} = \sim 1.3$ at 600 K

pure Pd, making it a cheaper potential alternative [109].

The separation factor of Pd with various binary hydrogen mixtures is shown in Fig. 5 [42]. There are two values for the separation factor for H/D mixtures due to the surface reactions (Eqn 1 and 2) [66]:



The separation factor for these two reactions is different and this gives rise to different values of α_{HD-H_2} and α_{D_2-HD} . The value of α_{HD-H_2} can be directly measured using dilute deuterium in protium, because it can be assumed all of the deuterium will be in the form of HD [66]. This concentration dependence has led to discrepancies in the reported α_{HD} value, and the deuterium concentration is not always reported [66,110].

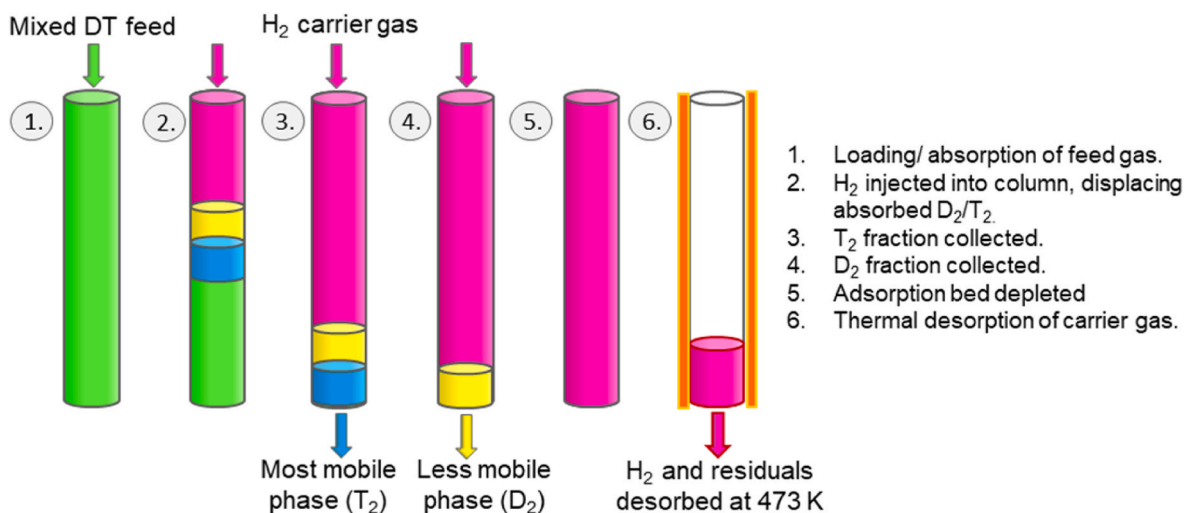


Fig. 4. –Hydrogen displacement chromatography cycle used to separate deuterium and tritium (not showing inter-fractions of DT, HT, HD also formed).

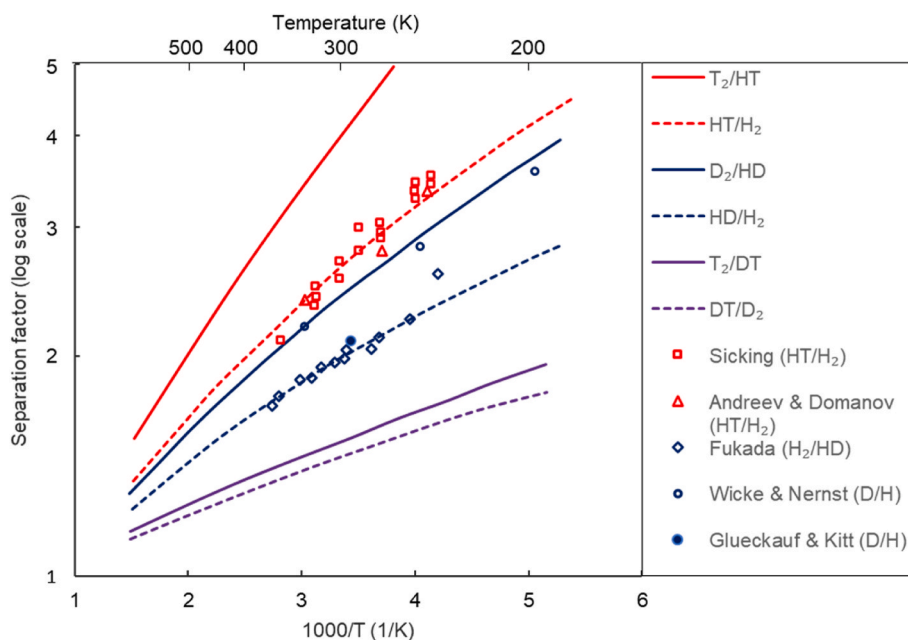


Fig. 5. Experimental and calculated values for the equilibrium absorption separation factor of palladium with different binary mixtures of hydrogen isotopes, data adapted from Horen & Lee [42] and updated with experimental data from Fukada et al. [66].

The separation factor α_{HD} is defined as follows [66,110]:

$$\alpha_{HD} = \frac{(2Y_{D_2} + Y_{HD})X_H}{(2Y_{H_2} + Y_{HD})X_D} \quad (3)$$

The terms relate to the respective concentrations of ($D_2/HD/H_2/H/D$) in the hydride phase (X) and the gas phase (Y). The separation factor can be related to isotherm data in the α , α - β (plateau region) and β phase [111] and has been used to analyse data obtained from a Sieverts-type volumetric apparatus [109,112,113].

In conclusion, GC is well suited to experimental scale isotope preparation because it can produce high purities and operate near ambient conditions. However, it has many significant drawbacks when applied at larger scales. The batch operation reduces the throughput capability and the requirement for palladium and high temperature regeneration increases the cost of the process. Vanadium and $LaNi_5$ based alloys have been tested, but their low performance compared to Pd means they are not currently viable alternatives. This may change as the cost of Pd

continues to rise. Adsorbents, which operate at cryogenic temperatures, may be advantageous due to their fast reaction kinetics and low cost.

4. Thermal Cycling Absorption Process (TCAP)

Thermal Cycling Absorption Process (TCAP) is based on the principle of Gas Chromatography and uses temperature cycling and flow reversal to achieve semi-continuous operation [114]. It is an application of parametric pumping where flow reversal is coupled to a parametric shift, such as temperature, electrochemical, pH, or electromagnetic [115,116]. TCAP processes have been in operation since 1994 at the Savannah River Site in the U.S [68,69].

TCAP uses a packed column, usually containing Pd coated on kieselguhr (Pd/k), connected to a gas storage vessel known as the reverser (see Fig. 6).

The TCAP cycle can be split into six key steps [42,69]:

Feeding – The column is initially at low pressure and low

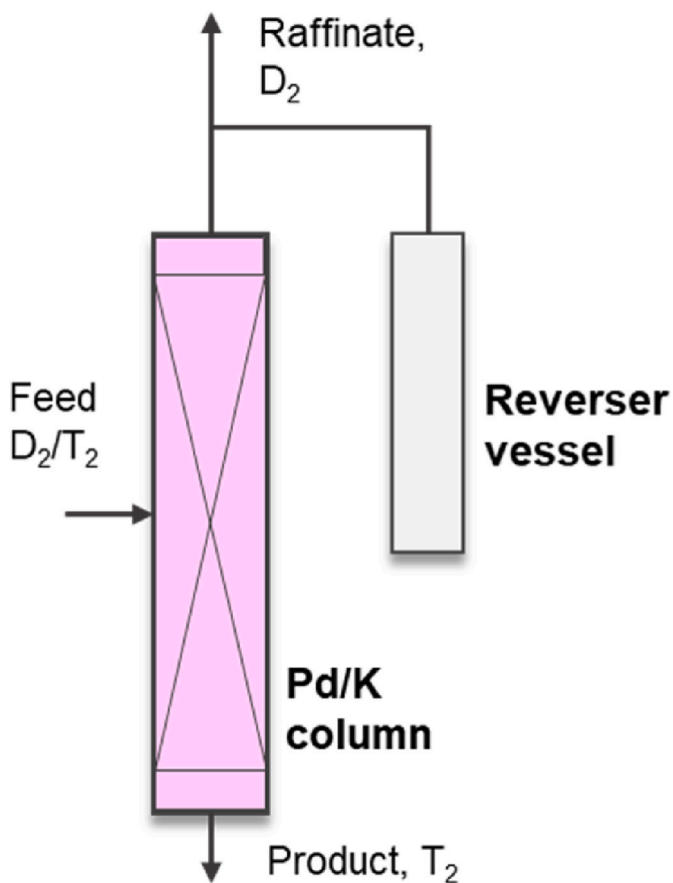


Fig. 6. Simplified diagram of TCAP consisting of a chromatographic separation column and holding column (the reverser). TCAP operation involves cycling the flow direction and column temperature.

temperature. The gas mixture is fed into the middle section of the column and equilibrates with the Pd/k packing.

Separating – Light isotopes in the reverser are passed down through the column. As in Gas Chromatography, the heavy isotopes are displaced from the Pd/k packing and move more quickly towards the bottom of the column. No bottom product is withdrawn at this stage.

Heating – The column is heated which causes desorption of the hydrogen isotopes. The pressure across the column rises.

Withdrawing – Product and raffinate streams are withdrawn from the top and bottom of the column respectively.

Desorbing – Light isotopes from the top of the column are passed back into the reverser vessel. This upward flow over Pd tends toward unwanted elution of heavy isotopes towards the top [42]. However, the higher temperature condition, minimises the unwanted chromatographic separation because of the lower separation factor and the low total hydrogen uptake.

Cooling – The column is cooled causing gas to be absorbed by the packing. The column is now ready for the next cycle.

Contamination from pipework is avoided because the light and heavy isotopes exit through different lines. Unlike Gas Chromatography the carrier gas in TCAP is composed of the gas mixture being separated which simplifies the process.

Ducet et al. [69] modelled the performance of a TCAP column and compared it to an experimental setup. They showed that the pressure significantly changes in response to the cycle operations and varies according to the position in the column. Yan et al. [117] conducted a dynamic simulation, suggesting optimal hot and cold operating temperatures in the TCAP cycle, and heating/cooling rates.

The TCAP design has low complexity, and is inherently suitable for

radioactive confinement [71]. Gas can repeatedly be processed in the same column to achieve high purities and near 100 % recovery [69,71]. The Pd on kieselguhr (Pd/k) packing material typically used for TCAP is heat treated to prevent mechanical breakdown of the particles [42,118].

Over recent decades TCAP has been further optimised for safety, efficiency and compactness [71]. Electric heaters and liquid nitrogen tubes have replaced the previous nitrogen gas heat transfer fluid and reduced the footprint of TCAP by an order of magnitude [119]. Another development is the replacement of the Plug Flow Reverser with an active inverse separation column using molecular sieves [120]. The combined Pd/k and inverse column operation enables the isotopes to be effectively separated twice which increases throughput and reduces the tritium inventory of the process [71,121].

TCAP has several advantages over conventional Gas Chromatography due to its semi-continuous operation, multi-cycle enrichment with high recovery, and the higher throughput per kg of Pd. The more efficient cycle will reduce the tritium processing time and column size, leading to lower tritium inventory for TCAP over Gas Chromatography. TCAP is adaptable since the lower operating temperature and the withdrawal rate of product can both be modified to cope with different isotope compositions and throughputs [69]. However, the requirement for liquid nitrogen cooling and electrical heating for each heating/cooling cycle makes the process quite energy intensive. TCAP is an attractive alternative to conventional separation methods at the demonstrated scale of a few moles per day [120,122], but scale-up may still be challenging especially with the high cost of Pd.

5. Palladium alloy membranes

Palladium (Pd) alloy membranes exhibit high permeability for hydrogen at elevated temperatures (573 – 773 K) [123]. Permeation of hydrogen through the membrane is driven by a pressure difference across the membrane. The high permeability coefficient means the process does not require high pressures and can be operated below atmospheric pressure which is beneficial as it limits tritium leakage to the outside. On the other hand, the elevated temperature accelerates tritium permeation through the stainless steel walls [124]. Membrane separation can operate continuously and does not require energy intensive temperature changes as for other processes that use Pd such as Gas Chromatography and TCAP.

The isotope selectivity from permeation through Pd membranes is determined by the isotope solubility, diffusion coefficient and the kinetics of the surface reaction (see Fig. 7) [125]. Despite the higher diffusion coefficient for heavier isotopes, the permeation rate is conversely highest for lighter isotopes. This is because the solubility of lighter isotopes is higher and so greater concentration differences drives the higher permeability. The H/D selectivity is approximately 2 at low *trans*-membrane pressure differences when surface reactions are limiting. At higher pressure differences, which is generally more optimal for operation due to greater membrane flux, the diffusion rate becomes limiting, and the selectivity drops to ~1.6.

In the diffusion-controlled regime, the separation factor for H/D has a weak dependence on temperature [123,125,126]. However, for D/T and H/T, the separation factor significantly increases as the temperature is reduced as shown in Fig. 8. If an alloy with high membrane flux at low temperatures could be developed, this high selectivity could be exploited [127]. It should be noted that some papers report very different temperature dependence of the H/D separation factor perhaps due to the low flow rates or reflux conditions used, which means that permeation may not be the rate limiting step [125,128].

The mass flux through a membrane, J ($\text{mol m}^{-2} \text{s}^{-1}$) can be related to permeability using the following simplified equation (Eqn 4) [129]:

$$J = \frac{\Phi(P_1^n - P_2^n)}{x} \quad (4)$$

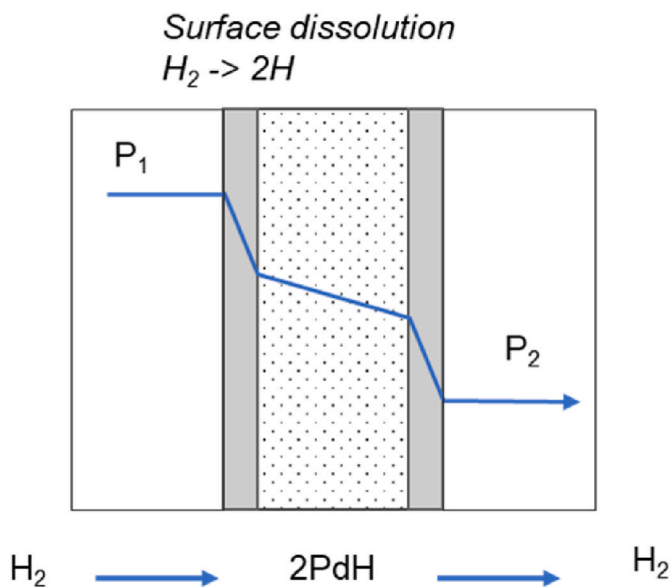


Fig. 7. Mass transfer of H_2 across a Pd membrane involving surface reaction and diffusion. Permeation driven by pressure difference across the membrane.

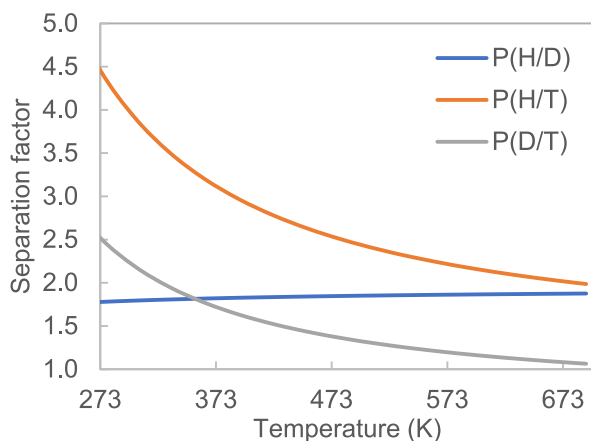


Fig. 8. Calculated temperature relations of the permeation (P) separation factor for Pd–Ag obtained from Nishikawa [126] and trends shown are in agreement with Evans et al. [127]. Permeation separation factor is the product of the diffusivity and solubility terms.

where Φ ($\text{mol m}^{-1} \text{s}^{-1} \text{Pa}^{-n}$) is the permeability coefficient, P_1 and P_2 are the partial pressures in the feed and permeate (Pa), x is the membrane thickness (m), and n is the partial pressure exponent. When n equals 0.5 the membrane obeys Sieverts' law which occurs at high pressure differences. At lower pressure differences, surface reactions of the gas molecules becomes the limiting step which causes the pressure exponent to tend towards a value of 1. Nishikawa et al. [126] reviewed literature data for hydrogen permeation rates and found that there was a wide pressure range where both surface reactions and diffusion significantly contributed to the overall permeation rate. This means the value of n can vary between 0.5 and 1. In the high pressure range, a value of above 0.5 can signify pinhole defects in the membrane [113]. The permeation rate tends to follow an exponential relation with temperature with surface reactions and diffusion rates both following an Arrhenius type relation, as discussed by Nishikawa et al. [126]. At lower temperatures (<373 K), surface oxide formation can significantly reduce permeability [126].

In Table 4, hydrogen permeability coefficients and separation factors have been compiled from literature studies for different dense metallic membrane materials. The permeability coefficient values have been

standardised by converting to a unit with a partial pressure exponent of 0.5 to enable comparison. Nishikawa et al. [126] makes the distinction between the ratio of isotopic effects between individual isotope experiments, termed $\beta_{H/D}$, also referred to as the ideal separation factor, and the actual separation factor of mixed isotope systems ($\alpha_{H/D}$). This distinction is also used in Table 4. In a supporting paper, the authors show that $\beta_{H/D}$ is appreciably lower than the separation factor [130].

Pd alloy membranes have been extensively tested and reviewed in the literature [129,139]. Pd alloys can have greater permeability, separation efficiency and mechanical properties over pure Pd [125,127]. The most common tested alloys are Pd–Ag [113,123,126] Pd–Y [125] and Pd–Cu. Pd–Ag is the most commonly studied alloy since it has approximately twice the hydrogen permeability of pure palladium. Pd–Cu has superior mechanical properties but normally has lower permeability than Pd–Ag or Pd–Y. Pati et al. [113] investigated $\text{Pd}_{0.77}\text{Ag}_{0.10}\text{Cu}_{0.13}$ and reported to have permeability rates of $12.6\text{--}14.8 \times 10^{-8} \text{ mol Pa}^{-0.5} \text{ m}^{-1} \text{ s}^{-1}$. However as can be seen in Table 4, Pati et al. [113] also reported very high values when testing Pd–Ag, much higher than standard literature values at similar temperatures (573 – 623 K). Ternary alloys like Pd–Cu–Ag may have some promising properties due to the segregation at the metal grain boundaries, and are beginning to be investigated further [140].

Pd–Y has the highest hydrogen permeability for Pd-alloys extending down to room temperature [129] and it may be possible to exploit the high selectivity for H/T and D/T at these temperatures [127]. The alloy is stable to air, since although Y_2O_3 forms on the surface, the oxide is not strongly bonded, so as Y is removed a stable active layer of Pd is left on the surface [141]. Luo et al. [125] measured the permeation rates for H–D–T mixtures through a Pd–Y alloy membrane. As discussed in the paper, the separation factors followed different trends with temperature to those predicted by the diffusion coefficient and solubility data. Wileman et al. [132] found the protium permeability rate for Pd–7.5%Y significantly increased when the temperature was increased above 573 K but this was not observed for deuterium, possibly due to an ordered-disordered state transition.

Pure Pd is not used for membranes since it becomes embrittled due to volume expansion during α – β hydride phase transition. One study produced a thin layer of pure Pd on a porous support that was resilient to α – β transition due to the thinness of the layer ($\sim 3 \mu\text{m}$) [133]. It was found that the α – β hydride phase transition could be independently controlled by adjusting pressure and temperature and this produced a significant increase in hydrogen flux. This also produced large isotopic differences in the individual components ($\beta_{H/D} = 7\text{--}8$) but not for mixed gases because both isotopes contribute to the phase transition.

The group-V metals (e.g. V, Nb, Ta) can have significantly higher permeability than Pd alloys but the rate of hydrogen dissociation on the surface is very low which limits the overall mass transfer. Formation of surface oxides also act as a barrier and the operating temperature is restricted due to hydrogen embrittlement at high pressures and lower temperatures [142,143]. Various alloys have been tested [142] such as V–Ni–Ti [144] which have improved permeability and ductility. Surface coatings such as TiC [135] and Mo_2C [143,145] can improve the rate of surface reaction and so significantly enhance permeation rates over uncoated vanadium. Pd-coated membranes such as Pd–V–Pd and Pd–Nb–Pd [146] can also achieve high permeability ($\sim 2 \times 10^{-6} \text{ mol m}^{-1} \text{ s}^{-1} \text{ Pa}^{-0.5}$ @ 623 K) but suffer from intermetallic diffusion above 673 K [135,143]. LaNi_5 on polyimide membranes have shown H/D separation factors as high as 1.9 but the permeation rate is extremely low [138]. Diffusion in LaNi_5 alloys is thought to be limited by a trapping phenomenon introduced by lattice defects [147]. Substituting Ni for other metals such as Al, is generally detrimental to the diffusion rate, though Co is an exception [147]. Overall, LaNi_5 and its derivative alloys are unlikely to be practical membrane materials due to the slow diffusion rate.

Glugla et al. [148] analysed the separation efficiency of a membrane system in the context of D/T separation for ITER. Optimal separation

Table 4
Hydrogen isotope separation studies for dense metallic membranes.

	Material-coating (atom% given in brackets)	H ¹ Permeability coefficient – 10 ⁻⁸ (mol Pa ^{-0.5} m ⁻¹ s ⁻¹) – (T/P conditions where available)	Separation factor (H/D unless stated otherwise) α = actual separation factor β = ideal separation factor	Thickness and coatings	T range (K)	Feed Pressure	Permeate pressure	Paper
Palladium alloys	Pd(75.3) Ag(24.7)	0.6 (373 K) - 1.8 (623 K)	β = 1.4 (373 K); 1.7 (623 K)	198 μm	323–773 K	1E-5 – 1 bar	Vac. (~0)	Serra [131]
	Pd(0.75)-Ag(0.25)	1.67 (623 K dP = 0.77–0.95 bar)	β = 1.64–2.00 (623 K)	100 μm	353–673 K	1.01 bar	0–1 bar	Nishikawa [126]
	Pd–Ag–Au	2.26 (623 K)	α(T/H) = 2.12 (623 K); 2.09 (823 K)	160 μm	623–823 K	n.g.	n.g.	Fujita [123]
	Pd(0.77)Ag(0.23) on porous stainless steel support	5.65–6.87 (n.g. T/°C.)	β = 1.30–1.41 (T n. g.)	100 μm	523–573 K	0.5–1.5 bar	Vac. (~0)	Pati [113]
	Pd(0.77)Ag(10)Cu (0.13) on porous stainless steel support	12.6–14.8 (n.g. T/°C)	β = 1.48–1.60 (T n. g.)	100 μm	523–573 K	0.5–1.5 bar	Vac. (~0)	Pati [113]
	Pd-(8.2 %)Y	n.g.	α = 1.43–1.38	80 μm	573–773 K	n.g.	n.g.	Luo [125]
	Pd–Y(7.5 %)	0.0942 (423 K) –5.65 (623 K)	β = 0.22 (423 K), 1.70 (623 K)	100 μm	373–753 K	7.8 bar	1 bar	Wileman [132]
	Pd–Ag–Y	n.g.	α = 1.30–1.32	"	573–773 K	n.g.	n.g.	Luo [125]
	Pd(91.31)Y(8.5)Ru (0.19)	0.94 (623 K)	α = 1.22	40 μm	573–723 K	>0.5 bar + perm' P	n.g.	Guangda [128]
	Stainless steel filter - Pd–Pd black	7.91 @ 423 K, 3 bar dP	β = 7–8 @ 423 K - α = 1.3 @ 423 K	100 μm	323–773 K	4–7 bar	1 bar	Aoki [133]
Pd	n.g.	α = 1.48 (HD in feed) α = 1.58 (HD not in feed)	400 μm	673 K	0.0267 bar	n.g.	Tanaka [134]	
TiC–V–TiC	n.g.	β = 1.34 (873 K); β = 1.15 (973 K °C)	100 μm V + 11.5–22.5 nm TiC	873–973 K	0.05–0.5 bar + perm' pressure	ng.	Fuerst [135]	
Vanadium alloys	Pd–V–Pd	145 (573 K) ^a	β = 1.50 (573 KC)	250 μm V +500 μm Pd	573 K	2–5 bar	1 bar	Dolan [136]
	Ni	3E-3 (723 K); 0.08 (1123 K)	β = 1.59 (723 K); β = 1.48 (1123 K)	1000 μm	723–1123 K	1 bar	n.g.	Noh [137]
Nickel and rare earth alloys	Ni/polyamide	1.5E-8 (368 K)	α = 2.0 (368 K)	0.75–1.0 μm	353–423 K	1.5 bar	n.g.	Sakaguchi [138]
	LaNi5/polyimide	3.2E-8 (368 K)	α = 1.9 (368 K)	0.75–1.0 μm	353–423 K	1.5 bar	n.g.	Sakaguchi [138]

^a Value obtained from fitting flux values and using total thickness of Pd and V.

Table 5

Theoretical gas diffusion separation factors calculated using equation 5.

Isotope mixture	Separation factor
H ₂ /D ₂	1.41
H ₂ /HD	1.22
D ₂ /T ₂	1.22
D ₂ /DT	1.11

efficiency for both the permeate and bleed streams, as a function of the separation factor and flow rates, occurred at about 1.7 times the breakthrough point, and efficiency quickly dropped away from this optimal point (see Fig. 9). The authors concluded that it would be difficult to maintain the membranes near their optimal efficiency point.

For multistage enrichment, cascade membrane designs have been investigated. Each stage would require its own control scheme to cope with changes in feed flow and composition [148]. Luo et al. [149] estimated the required membrane area for a membrane cascade design. Suzuki et al. [150] considered a continuous multistage membrane system with a single Pd alloy tube and counter-current feed and permeate flows. Membrane systems using counter-current or cross flows require only a single membrane and obtain higher separation efficiency than cascade systems. This is not well suited for producing high purity single

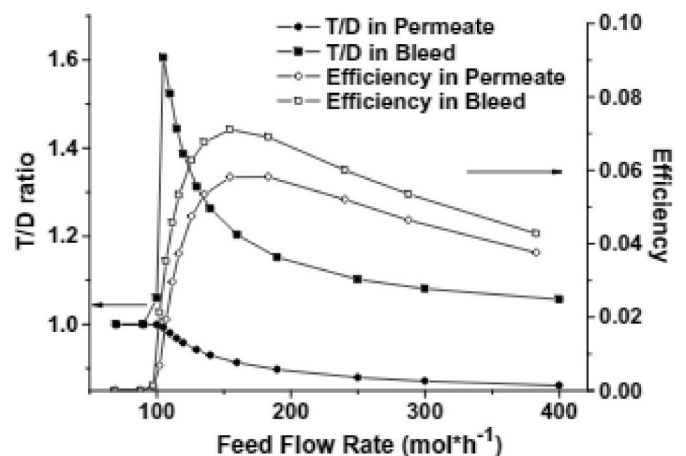


Fig. 9. Ratio of tritium/deuterium (T/D) and separation efficiency (see original paper for efficiency equation). Figure adapted with permission from Glugla et al. [148]. Values calculated for 1.99 % impurity concentration and feed and permeate pressures of 250 kPa and 10 kPa respectively.

isotopes but could work well for DT rebalancing in fusion energy plants.

Operational experience from the Savannah River Site demonstrated maintenance issues with membranes for tritium handling. Elevated temperatures deteriorated the seals and caused corrosion from the cooling water system [124]. An 'ageing' effect occurs due to the formation of He-3 bubbles arising from tritium decay, although these have been shown to have a negligible effect on the tensile strength at temperatures below 673 K [139,151,152]. Guangda et al. [128] measured significantly reduced permeation rates due to tritium ageing of PdY(8.5%)Ru(0.19%).

In conclusion, the continuous throughput capability, and the potential for high D/T selectivity near ambient temperatures makes Pd membranes attractive for scaled-up tritium processing. The key issues to address are the narrow operating range in cascade designs, and the high maintenance costs. Future studies could investigate modelling of alternative flow permeation system, and development of low temperature operating materials such as Pd-Y to make use of the potential for high D/T selectivity [127].

6. Non-metallic membranes

Porous membranes can allow gases to diffuse through driven by an applied pressure difference. The diffusion rate of a gas through a porous membrane is proportional to the square root of its molecular mass making it useful for isotope separation. Gas diffusion has long been used to separate isotopes of heavy elements for which it has a low selectivity. However, the high mass ratio between hydrogen isotopes results in more practical selectivity values. The maximum separation factor of gaseous diffusion is given by equation (5) and calculated for hydrogen isotope mixtures in Table 5 [153,154]:

$$\alpha = \frac{v_1}{v_2} = \sqrt{\frac{M_2}{M_1}} \quad (5)$$

where M_2 and M_1 are the molecular mass of the two gas components.

Gas diffusion benefits from low tritium inventory since only gaseous tritium is present in the process. It was selected by General Electric (GE) in their Trit*Ex® process design for concentrating tritium to 90% [155]. Other advantages are the simple start-up and shut down operation and mild operating temperatures. The main disadvantage is the low separation factor, and this means that a membrane cascade system is required to achieve significant enrichment. The GE design makes use of counter-current arrangement in each membrane cell as shown in Fig. 10. This produces a greater separation factor per membrane cell, however multiple compressors are required to drive the flow, and this means the number of units used for separation is very high.

Microporous zeolites [156,157] and silica-based materials [157] have the most potential for gas diffusion membranes, due to their small pore size, tritium compatibility and high hydrogen permeability. Table 6 shows that microporous ceramic membranes can achieve similar hydrogen flux to Pd alloys and so the required membrane areas for a certain throughput will be similar.

Table 6

Representative H₂ permeation through different membranes. Refer to equation 4.

Membrane type	Temperature/ °C	H ₂ permeability (units are as reported)	H ₂ flux at 1 bar pressure difference/mol m ⁻² s ⁻¹	Ref.
Microporous ceramic (zeolite)	150	~1 × 10 ⁻⁷ mol Pa ⁻¹ m ⁻² s ⁻¹	~0.01	[129, 157]
Pd alloy (PdAg _{0.25})	350	~2 × 10 ⁻⁸ mol Pa ^{-0.5} m ⁻¹ s ⁻¹	~0.06	[126, 131]
Dense polymers	95	~2 × 10 ⁻¹⁵ mol Pa ⁻¹ m ⁻¹ s ⁻¹	~8 × 10 ⁻⁶	[129]

Dense polymer membranes are common in commercial hydrogen purification but have low permeability [138]. Polymeric materials generally have poor tritium compatibility. Tritium can exchange with protium in the polymer chains and the beta radiation then causes incisions in the polymer chain [158]. Dense ceramic membranes would be more compatible with tritium but have low hydrogen flux [129].

Gas diffusion membranes avoid the high cost of Pd membranes, but they generally have low separation efficiency and are not likely to be competitive at large scales due to the large number of compressors and membrane cells required.

7. Electrochemical graphene membrane

An electrochemical setup using permeable 2D molecular sheets was first reported by a research group at the University of Manchester [159]. 2D molecular sheets such as graphene and boron nitride are permeable to thermal protons and electrons, but impermeable to larger molecular species (see Fig. 11). The protium ions (protons) pass more easily through the membrane than the heavier deuterium ions (deuterons). The researchers used a graphene sheet decorated with Pd or Pt nanoparticles attached to a proton permeable Nafion membrane. The separation factor was approximately 10 (8 for the larger membrane area due to defects), for both graphene and hexagonal boron nitride (hBN) 2D molecular sheets [159,160]. Subsequent studies by other authors have measured slightly higher separation factors of ~14 [161].

The mechanism of which protons can pass through 2D molecular sheets is still not well understood and is an area of on-going debate. An et al. [162] conducted a theoretical analysis, which suggested that atomic defects in the graphene sheet known as Stone-Wales defects, enable protons to penetrate the barrier. Yasuda et al. [163] measured the voltage dependence of the isotope selectivity and by comparing to theoretical calculations concluded that quantum tunnelling through the atomically thick graphene sheet is the mechanisms which causes the isotope selectivity. Other researchers suggest hydrogen chemisorbs between the C-C bonds and transfers to the other side of the graphene through a flipping mechanism [164,165]. Other papers suggest that the interaction with the catalyst causes the isotope selectivity with hydrogen transferring through defects through a mainly passive graphene layer [166].

The separation factor is of a similar order to high selectivity electrolysis [167,168], but the energy requirements for the graphene membrane are about 70% less than for electrolysis [169]. The graphene membrane can operate at 0.5 V while an alkaline electrolysis cell requires about 1.76 V. However, the use of both Pd and Pt in the membrane significantly increases the cost. Also, the reported proton flux is much lower than for standard membranes [160,170]. In units of current density, the graphene membrane flux is 0.064 A cm⁻² at 0.5 V, compared to ~1.5 A cm⁻² for PEM electrolysis and 0.5 A cm⁻² for alkaline electrolysis [170]. This low permeability rate will increase the required membrane area and processing time.

However, it is likely the performance of the graphene membrane could be significantly improved in future studies considering its early stage of development. The mechanism which enables proton transfer over the membrane it still not well understood, however alternative membrane materials may be able to achieve much greater membrane flux suitable for practical deuterium separation. For tritium applications in future fusion plants, the high tritium inventory of water and degradation of the Nafion membrane will be the major challenges.

8. Cryogenic distillation

Cryogenic distillation (CD) was used by Urey, Brickwede and Murphy in 1932 to isolate deuterium from natural hydrogen for the first time [171,172]. CD has been used throughout the development of fusion technology [11,173,174]: TSTA has been in operation since 1984 and was used to develop and demonstrate continuous tritium handling

Table 7
Experimental hydrogen inventory values for cryogenic distillation units.

System/Location	Packing type	Total system H inventory, (mol)	Liquid hold-up (mol/stage)	H Throughput (mol/h)	Ref
Experimental col. at TPL/JAERI (column 1)	Dixon rings	4.48	0.035	21.1	[9]
Princeton TFTR (4 column system)	n.g.	16.5	n.g.	3.43	[180, 181]
JET AGHS cryodistillation system (3 column system)	Dixon rings & spiral rings	77.1	0.04–0.08	14.0	[182]
Ontario Hydro experimental column	n.g.	~8.6 (column only)	0.118	n.g.	[177]
TSTA (column H)	Helipak	~15	0.0875	~18	[183]

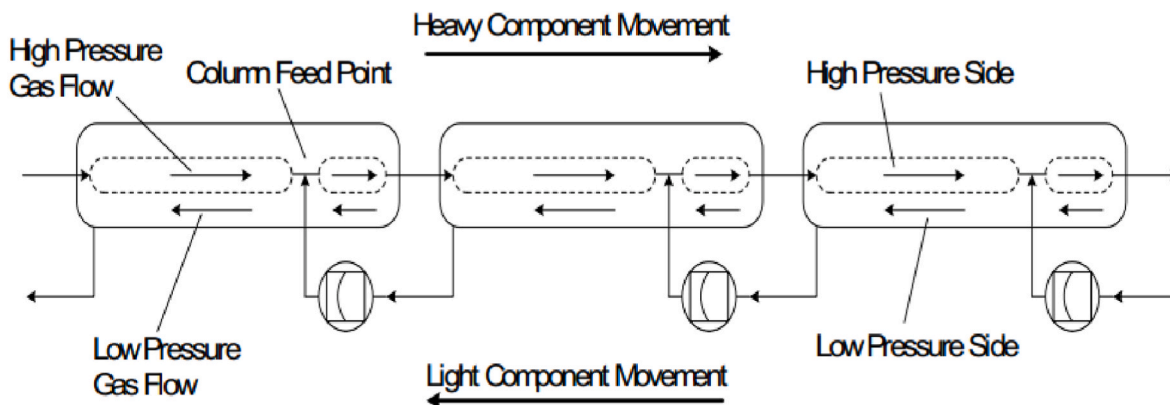


Fig. 10. Cascade membrane system for gas diffusion separation reprinted with permission from Ref. [155].

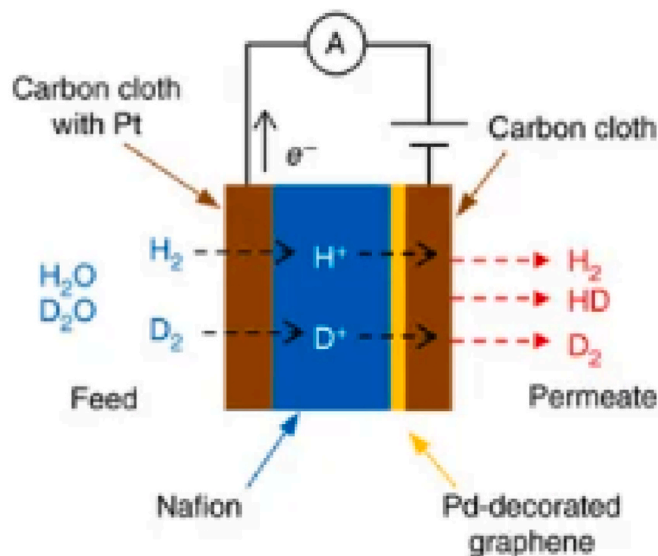


Fig. 11. Electrochemical pumping using graphene 2D molecular sheet reprinted with permission [159].

processes [11,175], and the Joint European Torus (JET) Active Gas Handling System also has a CD unit which began D_2 - T_2 experiments in 1995 [176]. The ITER isotope separation system will also use CD. CD has high tritium inventories due to the liquid hydrogen which is the main drawback for large scale use in future projects such as DEMO. One of the main focuses of this section is reviewing tritium inventory data from existing CD processes and research into reducing tritium inventory.

Cryogenic distillation (CD) separates hydrogen isotopes based on the difference in their vapour pressures. Assuming an ideal binary mixture of hydrogen isotopes, the separation factor can be determined from the relative volatility, shown in Fig. 12. Distillation columns are filled with a

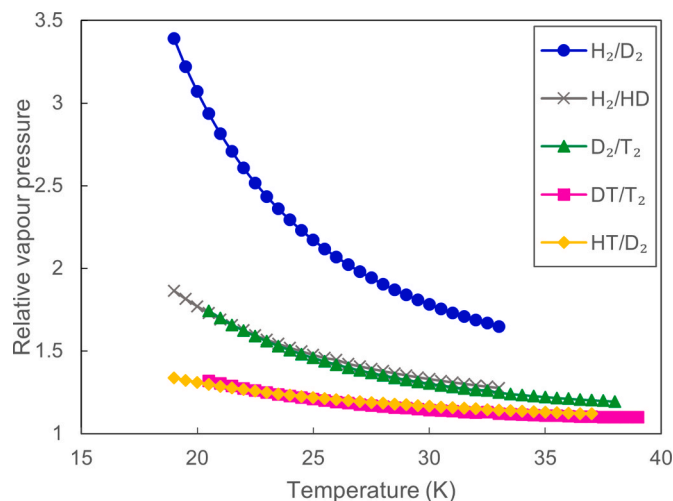


Fig. 12. Relative vapour pressure of ideal binary normal hydrogen isotope mixtures calculated as the ratio of the two component vapour pressures from source [6].

packing or trays which improve the contact between the liquid and vapour phases. Hydrogen distillation is conducted at temperatures between 20 and 26 K and near ambient pressures [9,177]. Refrigeration adds significant capital and operating costs and makes the process energy intensive. A realistic refrigeration system delivering 200 W of cooling power at 20 K can be expected to operate at only 0.75 % efficiency and so requires electrical power of at least 27 kW [178].

The JET CD system has three distillation columns connected in series and was designed to have an optimum daily output of 30 g T_2 (>99.989 %), 60 g D_2 (>99.998 %) and 150 g H_2 (>99.989 %) [75]. However, the system was never able to achieve this targeted performance since it could not produce the purity required. For ITER, a cascade of four distillation columns will be used for the isotope separation, which will

have an additional DT product for re-fuelling [14,179].

CD has a very high tritium inventory, mostly due to the liquid hold-up in the distillation column and liquid in other auxiliary units. Table 7 shows the measured system hydrogen inventory and liquid hold-up for some distillation systems reported in the literature. Approximate values of the average liquid residence time per stage were calculated by dividing the liquid hold-up per stage by the throughput of hydrogen isotopes. Values obtained of between 6 and 18 s for the three systems with available data show comparative performance.

Iwai et al. [183] experimentally measured the hydrogen inventory contributions for a column with HeliPak random packings and 80 theoretical stages, shown in Fig. 13. It suggests the packed section contains most of the hydrogen inventory. Other experimental studies suggest different contributions for the packed section. Operational data for the JET AGHS cryodistillation system has a liquid holdup in the packed sections (Dixon rings & spiral rings) that is only 21 % of the total [182] suggesting the condensers and reboilers contain a large portion of the hydrogen inventory. In another study by Iwai et al. [9] on a smaller experimental column with only 10 theoretical stages, the hydrogen inventory of the condenser was reported to be much higher than from the packed section (Dixon rings) or reboiler. These studies use similar packing types so instead the inconsistency could be due to different packing types so instead the inconsistency could be due to different reboiler/condenser designs, although this information is not reported.

The performance of a distillation column can be expressed numerically as the HETP (Height Equivalent to Theoretical Plate) [12,184]. The choice of column packing has a significant impact on the HETP, liquid holdup and flooding point [185,186]. Commercial random packings constructed of stainless-steel wire mesh are commonly used for hydrogen distillation due to their high performance [187]. Structured packings are not used in experimental columns perhaps since they are unavailable for small column diameter but could be important for future larger columns. Dixon rings, Coil pack, Heli-Pak and Helix type packings have been tested for H-D-T mixtures and gave HETP values of 4–6 cm. The Dixon ring packing provided the best combined performance in terms of low HETP, and a low pressure drop [187,188]. These packings are designed for conventional fluids such as water and hydrocarbons and a packing optimised for liquid hydrogen may be able to achieve improved performance and lower liquid hold-up [186]. Reported experimental HETP values for hydrogen isotopes are given in Table 8. One of the lowest HETP values of approximately 2.2 cm was obtained using spiral prismatic random packing (similar to Heli-Pak) which had been “pickled” in nitric acid to roughen the surface [189].

Safety is a major consideration of cryogenic distillation. Loss of power or cooling to the column can cause the liquid hydrogen in the column to quickly evaporate, and if unmitigated, will cause the pressure to rapidly rise beyond the maximum design limits [201]. ITER will need

to operate under a range of modes so system control must be able to cope with these variable demands [9]. Operation at 20–25 K presents many difficulties. Cool down may require days for large columns, and may never reach the required operating temperature without sufficient thermal shielding/insulation and cooling power [202].

Simulation can be used to estimate the tritium inventory and cooling requirements and analyse different column cascade configurations [11, 196,203]. The equilibrium stage model has been used by many groups as the basis to predict the steady state separation performance and dynamic response. The model has been applied to multicomponent mixtures containing all six isotopologues (H_2 , HD, D_2 , DT, T_2 and HT) and has been shown to accurately predict the steady state composition through the column but still requires experimental determination of HETP [197].

Early simulation studies found that the radioactive heat of tritium decay became significant at high tritium concentrations, causing the stripping column section to reach dryness unless the reflux rate was increased to compensate [11,204]. Some later models [12,205] also accounted for this heat of decay effect, but many other studies do not [9, 196,206]. Since it significantly affects the energy balance, discounting the heat of decay may be an inappropriate simplification that could lead to error. The value of specific heat of decay is 1.944 W/mol T_2 [11,12] and so a small D-T column with a tritium inventory of 2.24 mol [9] will have a total decay heat of approximately 4.35 W. This is of similar scale to the column reboiler power of 6 W which shows that tritium decay is expected to significantly affect the column performance as concluded in other studies [11,204]. Tritium decay heat is normally included in the energy balance of steady state models [12,204] but not in dynamic models [184,196] and can be seen in research papers where both steady state and dynamic models are reported [207].

Physical properties of liquid/vapour hydrogen isotopologues such as density or viscosity can be difficult to find as this data is generally not reported in simulation studies. The Twu-Alpha correlation used to correct the Peng Robinson equation of state has been shown to correct vapour pressure predictions for all hydrogen isotopologues. One study used averaged physical properties as a basis for prediction of wetting rates and liquid holdup but the validity of these empirical predictions is not certain for hydrogen systems [184].

Dynamic distillation models have been used in several studies to predict the response of the column to common process perturbations such as feed flow or composition [184,206] and develop control schemes for batch operated columns [208].

Studies have analysed potential failure scenarios such as loss of cooling or electrical power [201] and failure of the column to cool down to the operating temperature [202]. Models using ANSYS Fluent considered dynamic thermal effects of cold hydrogen gas entering the column which expands and accelerates under warming. Despite additional cooling in the middle of the column, it was still found that an additional radiation shield was needed for the entire column to reach 22 K [191].

In conclusion, experimental work has concentrated on testing overall column performance, and there is a lack of fundamental studies which investigate the interactions of hydrogen in the liquid/vapour phase with the packing surface [197]. This could inform the development of packing materials with lower HETP values and reduce the tritium inventory, and so help address the primary concern of cryogenic distillation for future fusion applications. So far, only commercially available stainless steel random packings have been tested. Due to the unique physical properties of hydrogen isotopes, development of specific packing materials could yield enhanced performance. There is also a need to develop accurate wetting and flooding correlations specifically for hydrogen systems. Safety of CD remains a concern despite improvements in this area and this will become more urgent as the scale of the technology increases. Research to minimise liquid inventory and improvements to safety instrumented systems will be of vital importance.

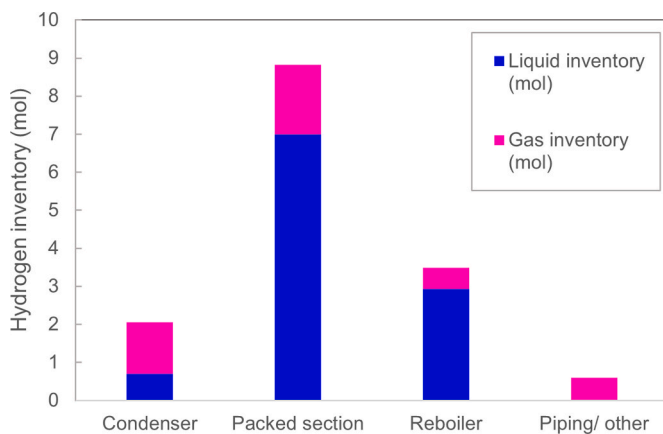


Fig. 13. Breakdown of tritium inventory from experimental data for cryogenic distillation column with HeliPak (4.4×2.3 mm) random packing and 80 theoretical stages [183].

Table 8

– Experimental studies on cryogenic distillation systems.

Institute	Packing type	HETP (cm)	Refrigeration power	Feed gas	Inner Column diameter (cm)	Packing (p) or Column (c) height (m)	N ^o of Stages	Column Temperature (K)	Column Pressure (kPa)	Ref.
ICIT, Rm. Valcea	Structured packings (ICIT B7) or random packings (sizes not given)	n.g.	1000 W @ 20 K	H ₂	10; 5; n.g.; 0.8	7 (tallest c)	n.g.	n.g.	150–350	[190, 191]
	Structured packings (ICIT B5 and B7) (sizes not given)	5.5 & 6.5	n.g.	D ₂ -nH ₂ -oH ₂	4.2	1.2 (p)	22	n.g.	150–350	[192, 193]
Petersburg Nuclear Physics Institute	Spiral prismatic random pack (2 × 2 mm)	2.2	20 W @ 20 K	H ₂ -HD	2.2	1.55 (p)	70	n.g.	120–900	[12, 189]
Osaka University; Institut de Physique Nucléaire et al.	Heli-Pak (2 × 2.5 mm)	2.9 ^a	6.3 W @ 10 K	H ₂ -HD-D ₂	3.2	1.10 (p)	38	17.5–20.5	n.g.	[194]
TRENTA (Tritium Lab Karlsruhe)	ng.	n.g.	250 W @ 20 K	D ₂ -DT-T ₂	4.0	4 (c)	n.g.	n.g.	n.g.	[195]
Los Alamos National Laboratory	ng.	5.08 ^a	n.g.	H-D-T	2.84	4 (p)	79	22–25	113–124	[196]
Japan Atomic Energy Research Institute	Dixon Ring (3 × 3 mm & 1.5 × 1.5 mm)	5	240 W @ 20 K	H-D-T	2.0 & 1.0	0.5 (p)	10	20–25	67–71	[9]
	Dixon Ring (3 × 3 mm)	4	n.g.	H-D-T	2.0	0.5 (p)	13	n.g.	80–83	[197]
Japan Atomic Energy Research Institute, Los Alamos National Laboratory	Dixon Ring (3 × 3 mm & 1.5 × 1.5 mm)	3–6	-	H-D-T	1 & 2	0.5 (p)	17	n.g.	n.g.	[188]
	Heli-Pak (4.4 × 2.3 mm)	4–6	n.g.	H-D-T	2.84 & 2.50	4.12 and 3.20 (p)	183	20–25	103	[198]
Japan Atomic Energy Research Institute	Dixon Ring (3 × 3 mm)	3–6	55 W @ 20 K	H ₂ -D ₂	1.84	0.5 (p)	17	20–25	40–200	[199]
	Dixon Ring (3 × 3 mm & 1.5 × 1.5 mm)	n.g.	240 W @ 20 K	n.g.	2 & 1	0.5 (p)	n.g.	20–25	48–152	[200]
	Dixon Ring, Coil Pack, Helix (3 × 3 mm) and Heli-Pak (2.5 × 1.25 mm)	5.5; 5.5; 6; & 6	55 W @ 20 K	N ₂ /Ar	1.94	0.5 (p)	9	n.g.	n.g.	[187]
JET, Culham UK	Dixon Ring & Spiral Rings (size not given)	6 & 7.5	200 W @ 20 K	H-D-T	1.6; 1.6; 17/13	4.80, 4.80, 6.90 (p)	260	18–26	100–121	[182]
Ontario Hydro Nuclear	ng.	2.05	53 W @ 24 K	D ₂ -DT	3.0	1.50 (p)	73	24	12	[177]
TSTA (Los Alamos Scientific Laboratory)	Commercial packings	5	450 W @ 20 K	H-D-T	2.9; 1.9; 2.3; 3.8	(C): 4.11, 4.06, 3.20, 4.11	310	n.g.	80–133	[11]

^a HETP values in these two studies are provided by the packing manufacturer.

9. Plasma-chemical separation

Plasma-chemical separation of hydrogen isotopes is based on the reversible chemical exchange between hydrogen gas and water vapour (Eqn 6) [209]:



The separation factor based on the chemical equilibrium is roughly 4 for H₂/HD [172] and 6.25 for H₂/HT [210] at 300 K. In this process a mixture of water vapour and hydrogen at atmospheric pressure and above 373 K is passed into a reaction chamber consisting of micro-hollow alumina channels held between two metal electrodes. The discharging electrodes creates a plasma which generates highly reactive species that enables exchange reactions to occur between hydrogen and water molecules. The plasma-chemical method demonstrates very fast deuterium transfer kinetics and the rate constant is an order of magnitude higher than conventional platinum catalysts. This enables the reaction to occur in very small chambers which leads to lower tritium inventory.

The main drawback compared to platinum catalysts is the additional energy required to vaporise the water and generate the plasma, the latter was estimated to be 3.6 kJ per mole of water [209]. While the rapid kinetics bring some benefits, the plasma-chemical exchange would need

to be coupled to a phase change process such as electrolysis which would further increase the energy demand. This is similar to the Combined Electrolysis Catalytic Exchange (CECE) process which is detailed in the appendix. The electrolysis unit would account for significant tritium inventory. In this arrangement the plasma-chemical separation would have high total tritium inventory due to the contributions from the electrolyser and additional water processing units. It may be possible to use a bi-thermal arrangement of two plasma-chemical reactors, similar to the Girdler-Sulphide (GS) process (see appendix), which would negate the requirement for phase changes and reduce tritium inventory. However more work is required to analyse the possibility of these two arrangements. Since the original papers in 2005, there have been no further publications in the open literature on the plasma-chemical process.

The potential of this process for very low tritium inventories and high equilibrium separation factor could offset its high electrical energy requirements. This would make it of interest for future fusion plant applications. However, it is still at an early stage of development and auxiliary units required to process the water such as electrolysers, condensers, and purifiers may negate its fundamental advantage of low tritium inventory.

10. Thermal diffusion

When a temperature gradient is applied to a gaseous isotope mixture, the lighter isotopes tend to accumulate at the hot side, due to the thermal diffusion effect. Thermal diffusion was first developed into an isotope separation process by Clusius & Dinkel over 100 years ago and the design concept hasn't changed much since then [211,212]. In this design, a temperature gradient is maintained in the radial direction between two concentric cylinders: the inner cylinder is normally heated to high temperature, often using an electrically heated wire. The outer cylinder is maintained at low temperature using liquid cooling with either water or liquid nitrogen. The thermal diffusion effect causes a radial flow of the lighter isotopes towards the hot inner. Thermal convection currents produce a countercurrent axial flow in the column enabling multiple separation stages in a single column. The flow must remain laminar which limits the column size. Undesirable secondary circulation systems can develop in tall thermal diffusion columns, causing remixing which reduces the separation efficiency [213,214]. Multiple short columns can be connected in series to reduce remixing effects and improve separation efficiency [215,216]. The separation factor depends upon the thermal diffusion factor, diffusivity and viscosity of the gas, as well as the flow regime in the column [217].

Thermal diffusion is often used in small and medium scale applications because of its simple design, low tritium inventory, and high separation factor. There is minimal contact of the treated gas with solid materials which makes it suitable for tritium processing. Start-up times are very quick, and steady state operation can be reached within 20–30 min [218]. For large scale applications, the low thermodynamic efficiency and low throughput make it less competitive with alternative processes [211]. The thermal diffusion units used at the Savannah River Site were gradually replaced by Cryogenic Distillation from 1967, and later by TCAP [71,219]. Thermal diffusion was used by the Japan Atomic Energy Research Institute for tritium recovery and enrichment in the 1980–90s [217].

The maximum separation factor is exponentially related to the ratio of the temperature difference between the hot and cold walls to the cold wall temperature. Accordingly, a cryogenically cooled column would improve the separation efficiency over the water-cooled device and recent studies have explored this effect [216], often using liquid nitrogen temperature [217]. The cryogenic wall separation factor can be 4 to 10 times higher than the water-cooled process ($T_C = \sim 288$ K) [217,220].

The temperature of the heating wire is also important. Using high temperatures such as 1073 K, the heteromolecules equilibrium reactions are fast which enables more efficient preparation of high purity isotope products without external equilibrators [220]. However, a high temperature heating wire could be an ignition hazard leading to safety concerns in either event of a leak or loss of containment. Using heating temperatures below hot surface ignition temperature (as low as 620 K at reduced pressure [221]) would lessen this risk but reduce separation efficiency.

The cryogenic wall adaptation could improve the suitability of thermal diffusion for small-scale applications. However, it is unlikely to be viable for large scale applications in future fusion plants due to the low thermodynamic efficiency, limitations of the column size and safety concerns.

11. Laser isotope separation

Laser isotope separation utilises the selective adsorption of photons by atoms and molecules of different isotopes at discrete frequencies. This method can achieve very high selectivity ($>10^4$) and can reach high levels of enrichment from extremely dilute hydrogen isotope mixtures [222]. In small atoms such as hydrogen, the presence of extra neutrons in the nucleus causes a shift in the electronic energy levels which shifts the frequency of photons which can be adsorbed. Thus, it is possible to excite the atoms or molecules containing a specific isotope with high

selectivity. Lasers are an extremely convenient source of high intensity monochromatic light which provide a long optical path and pulse length modulation [223].

Laser isotope separation can be divided into two categories, depending on if the process uses atomic hydrogen or molecular hydrogen. The first category is Atomic Vapour Laser Isotope Separation (AVLIS) which uses lasers to selectively ionise atoms of different isotopes which are then separated using an electric field [223]. It is used to separate the isotopes of heavy elements, however the high cost and complexity of the AVLIS laser and collector systems mean it is unlikely to be competitive for hydrogen isotopes [224].

The second category is Molecular Laser Isotope Separation (MLIS) which uses lasers to selectively excite isotope containing molecules which drives a photochemical reaction, photoionization or photodissociation [223]. MLIS then uses a chemical separation to recover the reaction products and therefore does not require a complex collection system as for AVLIS. Also, by choosing a suitable molecule that adsorbs light of a certain wavelength, the process can use commercially available laser sources which are much cheaper. Many processes use multi-photon absorption to provide the molecules with enough energy in the IR-visible-UV range [223]. The selection of a suitable molecule for MLIS is based on the yield, the isotopic selectivity of the multi-photon dissociation, the required laser source to produce the correct wavelength and the cost of the chemical compound [222]. For hydrogen isotope separation, one of the most extensively investigated processes is the multiphoton photodissociation of halogenated organic compounds such as trifluoromethane [225], chloroform [226] and pentafluoroethane [225].

In the first step, these molecules must be exchanged with the source of hydrogen isotopes. This is achieved in a base catalysed exchange reaction with water (Eqn 7) [225,227]:



This reaction can be slow especially for fluoroalkanes, which may limit throughput and increase the tritium inventory in the exchange column.

After the exchange process, the compounds are irradiated with the laser. Laser excitation of gaseous feeds generally requires low pressure (100–1000 Pa) to prevent collisions between the excited molecules and ground state, but laser pulses can be used to maintain selectivity at relatively higher pressures (~ 1300 Pa) [226,228]. Liquid samples can be used but may need to be cooled to improve the resolution of the spectral adsorption features [229]. Photodissociation has demonstrated very high selectivity of over 5000 for a range of compounds and laser sources. Furthermore, by altering the laser frequency, it is possible to selectively photo-dissociate protium, deuterium or tritium in the sample even at very low concentrations, making it potentially highly adaptable. However, the chemical products from these reactions such as HF and C_2F_2 can be extremely difficult to use in a process due to their toxicity and chemical incompatibility.

Photo-dissociation of fluoroalkanes can be achieved using commercially available CO_2 lasers in the near-IR range [222]. Other processes may require different laser frequencies, using alternative laser sources or tuneable dye laser sources which are more expensive and less efficient [230]. Other molecules have been investigated for photodissociation such as formaldehyde [230,231] and chloroform [227]. Isotope selective laser-induced reaction of bromine with alkanes using a carbon dioxide sensitizer [232], and methanol [233] has also been described. Mayer et al. was reported to enrich a 1:1 mixture of $H_3COH:D_3COD$ to greater than 95 % D_3COD using a hydrogen fluoride laser [233].

The operating costs and capital costs of MLIS are expected to be high, due to the use of high-performance lasers, vacuum conditions and additional process equipment. One advantage of this process is that it can be conducted at ambient temperatures and low hydrogen pressures, making the process safer and easier to operate. Due to its high isotope

selectivity, MLIS would be well suited to recovering low concentrations of hydrogen isotopes. However, the slow initial exchange reaction would limit the potential throughput. It may be possible to develop faster isotope exchange catalysts for example, platinum which is used in chemical exchange. Indeed, MLIS could be beneficial in combination with conventional chemical exchange reactions (see appendix) providing additional separation and acting as a phase change process to the exchange column. MLIS has a lot of potential if a suitable photochemical process can be developed which uses standard laser sources and easy to handle chemicals and if it can be linked to a fast isotope exchange process. Advances in laser technology may enable other excitation molecules to be used.

12. Conclusions

In recent years, new processes and mechanisms for hydrogen isotope separation have been developed which show high selectivity over conventional processes and potentially have advantages making them suitable for different applications.

For the enrichment of deuterium, electrochemical membranes using graphene are reported to have a high separation factor and permeability with much lower electrical demand than electrolysis. Laser isotope separation could also be effective if a suitable photochemical system could be developed. It is noted that in laser isotope separation, the kinetics of the chemical exchange step is likely to limit throughput, but chemical exchange could provide added separation performance, an important consideration for future studies.

For future fusion energy, high throughput isotope separation is required at much reduced tritium inventory compared to conventional techniques. Research into adsorbent materials has produced materials with some of the highest isotope selectivity and when scaled-up using a PSA type adsorption cycle this would enable high throughput and efficiency with low tritium inventory. Plasma-chemical separation is at an early stage of development but is an interesting candidate due to the potential for extremely low tritium inventories and high selectivity. More work is required to analyse plasma-chemical processes including the auxiliary units which may negate the benefits of this process. For cryogenic distillation to be competitive with these new techniques, the tritium inventory needs to be significantly reduced. Future research should investigate bespoke packing shapes designed for hydrogen isotope fluids with low liquid hold-up. Cryogenic distillation may still be the most suitable technique for the protium removal step in the inner fuel loop, due to its capability of removing low concentrations of hydrogen isotopes.

For low tritium concentration applications such as tritium recovery and tritium removal from waste streams, high selectivity and energy efficiency are more important than low tritium inventory and throughput capability. Thermal Cycling Adsorption Process (TCAP) may be well suited for tritium extraction due to its semi-continuous operation and multi-cycle enrichment capability. Palladium membranes have tritium selectivity which is significantly enhanced at room temperature compared to conventional membrane temperatures (623 K). If a palladium alloy could be developed with high permeability at room temperature, then this could be highly effective for tritium recovery and would solve maintenance issues caused by high temperatures. Pd–Y and ternary Pd alloys show some promise and should be investigated further. As demonstrated in this article, several technologies are emerging that could be developed into efficient alternatives for hydrogen isotope separation and solve one of the key challenges for future commercial fusion energy.

Declaration of competing interest

The authors declare that they have no known competing financial interests or personal relationships that could have appeared to influence the work reported in this paper.

Acknowledgments

This research is supported by the UK Atomic Energy Authority (UKAEA) and the H3AT division.

Appendix A. Supplementary data

Supplementary data to this article can be found online at <https://doi.org/10.1016/j.ijhydene.2023.10.282>.

References

- [1] IEA. World Energy outlook 2019. Paris: IEA; 2019.
- [2] UNFCCC. The Paris Agreement. 2020.
- [3] Lawless R, Butler B, Hollingsworth A, Camp P, Shaw R. Tritium plant technology development for a DEMO power plant. *Fusion Sci Technol* 2017;71:679–86.
- [4] Shaw RCR, Butler B. Applicability of a cryogenic distillation system for D-T isotope rebalancing and protium removal in a DEMO power plant. *Fusion Eng Des* 2019;141:59–67.
- [5] Usdo Energy. Tritium handling and safe storage. Washington; 2015.
- [6] Roder HM, Childs GE, McCarty RD, Angerhofer PE. Survey of the properties of the hydrogen isotopes below their critical temperatures. United States. National Bureau of Standards.; 1973.
- [7] Lemmon EW, McLinden MO, Friend D. Thermophysical properties of fluid systems. In: Linstrom PJ, Mallard WG, editors. NIST chemistry WebBook, NIST standard reference database number 69: Gaithersburg MD.
- [8] Jacobs DG. Sources of tritium and its behavior upon release to the environment. United States: AEC Critical Review Series; 1968.
- [9] Iwai Y, Yamanishi T, O'Hira S, Suzuki T, Shu WM, Nishi M. H-D-T cryogenic distillation experiments at TPL/JAERI in support of ITER. *Fusion Eng Des* 2002; 61–62:553–60.
- [10] Lässer R, Klatt KH. Solubility of hydrogen isotopes in palladium. *Phys Rev B* 1983;28:748–58.
- [11] Bartlit JR, Sherman RH, Stutz RA, Denton WH. Hydrogen isotope distillation for fusion power reactors. *Cryogenics* 1979;19:275–9.
- [12] Alekseev I, Arkhipov E, Bondarenko S, Fedorchenko O, Ganzha V, Ivshin K, et al. Cryogenic distillation facility for isotopic purification of protium and deuterium. *Rev Sci Instrum* 2015;86:125102.
- [13] Neugebauer C, Hörstemsmeier Y, Day C. Technology development for isotope rebalancing and protium removal in the EU-DEMO fuel cycle. *Fusion Sci Technol* 2020;76:215–20.
- [14] Abdou M, Riva M, Ying A, Day C, Loarte A, Baylor LR, et al. Physics and technology considerations for the deuterium–tritium fuel cycle and conditions for tritium fuel self sufficiency. *Nucl Fusion* 2020;61:013001.
- [15] Federici G, Boccaccini L, Cismondi F, Gasparotto M, Poitevin Y, Ricapito I. An overview of the EU breeding blanket design strategy as an integral part of the DEMO design effort. *Fusion Eng Des* 2019;141:30–42.
- [16] Day C, Butler B, Giegerich T, Ploeckl B, Varoutis S. A smart three-loop fuel cycle architecture for DEMO. *Fusion Eng Des* 2019;146:2462–8.
- [17] Beenakker JJM, Borman VD, Krylov SY. Molecular transport in subnanometer pores: zero-point energy, reduced dimensionality and quantum sieving. *Chem Phys Lett* 1995;232:379–82.
- [18] Zhang L, Wulf T, Baum F, Schmidt W, Heine T, Hirscher M. Chemical affinity of Ag-exchanged zeolites for efficient hydrogen isotope separation. *Inorg Chem* 2022;61:9413–20.
- [19] Xiong R, Chen J, Zhang L, Li P, Yan X, Song Y, et al. Hydrogen isotopes separation in Ag(I) exchanged ZSM-5 zeolite through strong chemical affinity quantum sieving. *Microporous Mesoporous Mater* 2021;313:110820.
- [20] Bezverkhy I, Giraudet M, Dirand C, Macaud M, Bellat J-P. Enhancement of D2/H2 selectivity in zeolite A through partial Na–K exchange: single-gas and coadsorption studies at 45–77 K. *J Phys Chem C* 2020;124:24756–64.
- [21] Taguchi A, Nakamori T, Yoneyama Y, Sugiyama T, Tanaka M, Kotoh K, et al. Hydrogen isotope (H2 and D2) sorption study of CHA-type zeolites. *Fusion Sci Technol* 2020;76:314–20.
- [22] Kawamura Y, Iwai Y, Munakata K, Yamanishi T. Effect of cation exchange on hydrogen adsorption property of mordenite for isotope separation. *J Nucl Mater* 2013;442:S455–60.
- [23] Giraudet M, Bezverkhy I, Weber G, Dirand C, Macaud M, Bellat J-P. D2/H2 adsorption selectivity on FAU zeolites at 77.4 K: Influence of Si/Al ratio and cationic composition. *Microporous Mesoporous Mater* 2018;270:211–9.
- [24] Bezverkhy I, Boyer V, Cabaud C, Bellat J-P. High efficiency of Na- and Ca-exchanged chabazites in D2/H2 separation by quantum sieving. *ACS Appl Mater Interfaces* 2022;14:52738–44.
- [25] Kotoh K, Kudo K. Multi-component adsorption behavior of hydrogen isotopes on zeolite 5A and 13X at 77.4 K. *Fusion Sci Technol* 2005;48:148–51.
- [26] Xiong R, Balderas Xicohtencatl R, Zhang L, Li P, Yao Y, Sang G, et al. Thermodynamics, kinetics and selectivity of H2 and D2 on zeolite 5A below 77K. *Microporous Mesoporous Mater* 2018;264:22–7.
- [27] Kotoh K, Kimura K, Nakamura Y, Kudo K. Hydrogen isotope separation using molecular sieve of synthetic zeolite 3A. *Fusion Sci Technol* 2008;54:419–22.

- [28] Muhammad R, Jee S, Jung M, Park J, Kang SG, Choi KM, et al. Exploiting the specific isotope-selective adsorption of metal-organic framework for hydrogen isotope separation. *J Am Chem Soc* 2021;143:8232–6.
- [29] Oh H, Savchenko I, Mavrandonakis A, Heine T, Hirscher M. Highly effective hydrogen isotope separation in nanoporous metal-organic frameworks with open metal sites: direct measurement and theoretical analysis. *ACS Nano* 2014;8:761–70.
- [30] Ha J, Jung M, Park J, Oh H, Moon HR. Thermodynamic separation of hydrogen isotopes using hofmann-type metal-organic frameworks with high-density open metal sites. *ACS Appl Mater Interfaces* 2022;14:30946–51.
- [31] Si Y, He X, Jiang J, Duan Z, Wang W, Yuan D. Highly effective H₂/D₂ separation in a stable Cu-based metal-organic framework. *Nano Res* 2021;14:518–25.
- [32] Zhang L, Jee S, Park J, Jung M, Wallacher D, Franz A, et al. Exploiting dynamic opening of apertures in a partially fluorinated MOF for enhancing H₂ desorption temperature and isotope separation. *J Am Chem Soc* 2019;141:19850–8.
- [33] Mondal SS, Kreuzer A, Behrens K, Schütz G, Holdt H-J, Hirscher M. Systematic experimental study on quantum sieving of hydrogen isotopes in metal-amide-imidazolate frameworks with narrow 1-D channels. *ChemPhysChem* 2019;20:1311–5.
- [34] FitzGerald SA, Pierce CJ, Rowsell JLC, Bloch ED, Mason JA. Highly selective quantum sieving of D₂ from H₂ by a metal-organic framework as determined by gas manometry and infrared spectroscopy. *J Am Chem Soc* 2013;135:9458–64.
- [35] Kim JY, Balderas-Xicohtencatl R, Zhang L, Kang SG, Hirscher M, Oh H, et al. Exploiting diffusion barrier and chemical affinity of metal-organic frameworks for efficient hydrogen isotope separation. *J Am Chem Soc* 2017;139:15135–41.
- [36] Han G, Gong Y, Huang H, Cao D, Chen X, Liu D, et al. Screening of metal-organic frameworks for highly effective hydrogen isotope separation by quantum sieving. *ACS Appl Mater Interfaces* 2018;10:32128–32.
- [37] Oh H, Park KS, Kalidindi SB, Fischer RA, Hirscher M. Quantum cryo-sieving for hydrogen isotope separation in microporous frameworks: an experimental study on the correlation between effective quantum sieving and pore size. *J Mater Chem A* 2013;1:3244–8.
- [38] Sugiyama H, Hattori Y. Quantum-molecular sieving of hydrogen isotopes in fluorinated carbon nanopores. *Chem Lett* 2021;50:1460–3.
- [39] Chu X-Z, Cheng Z-P, Xiang X-X, Xu J-M, Zhao Y-J, Zhang W-G, et al. Separation dynamics of hydrogen isotope gas in mesoporous and microporous adsorbent beds at 77 K: SBA-15 and zeolites 5A, Y, 10X. *Int J Hydrogen Energy* 2014;39:4437–46.
- [40] Krkljus I, Steriotis T, Charalambopoulou G, Gotzias A, Hirscher M. H₂/D₂ adsorption and desorption studies on carbon molecular sieves with different pore structures. *Carbon* 2013;57:239–47.
- [41] Hu X, Ding F, Xiong R, An Y, Feng X, Song J, et al. Highly effective H₂/D₂ separation within the stable Cu(I)Cu(II)-BTC: the effect of Cu(I) structure on quantum sieving. *ACS Appl Mater Interfaces* 2023;15:3941–52.
- [42] Horen AS, Lee MW. Metal hydride based isotope separation – large-scale operations. *Fusion Technol* 1992;21:282–6.
- [43] Kim JY, Zhang L, Balderas-Xicohtencatl R, Park J, Hirscher M, Moon HR, et al. Selective hydrogen isotope separation via breathing transition in MIL-53(Al). *J Am Chem Soc* 2017;139:17743–6.
- [44] Oh H, Hirscher M. Quantum sieving for separation of hydrogen isotopes using MOFs. *Eur J Inorg Chem* 2016;2016:4278–89.
- [45] FitzGerald SA, Burkholder B, Friedman M, Hopkins JB, Pierce CJ, Schloss JM, et al. Metal-specific interactions of H₂ adsorbed within isostructural metal-organic frameworks. *J Am Chem Soc* 2011;133:20310–8.
- [46] Weinrauch I, Savchenko I, Denysenko D, Souliou SM, Kim HH, Le Tacon M, et al. Capture of heavy hydrogen isotopes in a metal-organic framework with active Cu (I) sites. *Nat Commun* 2017;8:14496.
- [47] Flanagan TB, Luo W, Clewley JD. Calorimetric enthalpies of absorption and desorption of protium and deuterium by palladium. *J Less Common Metals* 1991;172–174:42–55.
- [48] Wilson J, Becnel J, Demange D, Rogers B. The ITER tokamak exhaust processing system design and substantiation. *Fusion Sci Technol* 2019;75:794–801.
- [49] Kotoh K, Takashima S, Sakamoto T, Tsuge T. Multi-component behaviors of hydrogen isotopes adsorbed on synthetic zeolites 4A and 5A at 77.4K and 87.3K. *Fusion Eng Des* 2010;85:1928–34.
- [50] Physick AJW, Wales DJ, Owens SHR, Shang J, Webley PA, Mays TJ, et al. Novel low energy hydrogen-deuterium isotope breakthrough separation using a trapdoor zeolite. *Chem Eng J* 2016;288:161–8.
- [51] Xiong R, Zhang L, Li P, Luo W, Tang T, Ao B, et al. Highly effective hydrogen isotope separation through dihydrogen bond on Cu(I)-exchanged zeolites well above liquid nitrogen temperature. *Chem Eng J* 2020;391:123485.
- [52] Thomas WJ, Crittenden B. Adsorption technology and design. Oxford: Butterworth-Heinemann; 1998.
- [53] Sircar S, Golden TC. Purification of hydrogen by pressure swing adsorption. *Separ Sci Technol* 2000;35:667–87.
- [54] Kotoh K, Tanaka M, Takashima S, Tsuge T, Asakura Y, Uda T, et al. Verification of hydrogen isotope separation by pressure swing adsorption process: successive volume reduction of isotopic gas mixture using SZ-5A column. *Fusion Eng Des* 2011;86:2799–804.
- [55] Kotoh K, Tanaka M, Tsuge T, Moriyama S, Takashima S, Asakura Y, et al. Successive hydrogen isotope separation/enrichment by pressure swing adsorption using SZ-13x column. *Fusion Sci Technol* 2011;60:1355–8.
- [56] Kotoh K, Tanaka M, Nakamura Y, Sakamoto T, Asakura Y, Uda T, et al. Experimental verification of hydrogen isotope separation by pressure swing adsorption. *Fusion Sci Technol* 2008;54:411–4.
- [57] Lei Q-H, Tang T, Xiong Y-F, Zhang G-H, Qin C, Huang Z-Y, et al. Experimental verification of hydrogen isotope enrichment process by dual-column pressure swing and temperature swing adsorption. *Fusion Eng Des* 2021;172:112726.
- [58] Wong YW, Hill FB, Chan YNL. Studies of the separation of hydrogen isotopes by a pressure swing adsorption process. *Separ Sci Technol* 1980;15:423–55.
- [59] Fitzgerald SA, Shinbrough K, Rigdon KH, Rowsell JLC, Kapelowski MT, Pang SH, et al. Temperature-programmed desorption for isotope separation in nanoporous materials. *J Phys Chem C* 2018;122:1995–2001.
- [60] Bezverkhy I, Pujol Q, Dirand C, Herbst F, Macaud M, Bellat J-P. D₂ and H₂ adsorption capacity and selectivity in CHA zeolites: effect of Si/Al ratio, cationic composition and temperature. *Microporous Mesoporous Mater* 2020;302:110217.
- [61] Bondorf L, Fiorio JL, Bon V, Zhang L, Maliuta M, Ehrling S, et al. Isotope-selective pore opening in a flexible metal-organic framework. *Sci Adv* 2022;8:eabn7035.
- [62] Li X, Wang X, Li M, Luo J, An Y, Li P, et al. Highly selective adsorption of D₂ from hydrogen isotopes mixture in a robust metal bistriazolate framework with open metal sites. *Int J Hydrogen Energy* 2020;45:21547–54.
- [63] Teufel J, Oh H, Hirscher M, Wahiduzzaman M, Zhechkov L, Kuc A, et al. MFU-4 – a metal-organic framework for highly effective H₂/D₂ separation. *Adv Mater* 2013;25:635–9.
- [64] Oh H, Kalidindi SB, Um Y, Bureekaew S, Schmid R, Fischer RA, et al. A cryogenically flexible covalent organic framework for efficient hydrogen isotope separation by quantum sieving. *Angew Chem Int Ed* 2013;52:13219–22.
- [65] He D, Zhang L, Liu T, Clowes R, Little MA, Liu M, et al. Hydrogen isotope separation using a metal-organic cage built from macrocycles. *Angew Chem Int Ed* 2022;61:e202202450.
- [66] Fukada S, Fuchinoue K, Nishikawa M. Isotope separation factor and isotopic exchange rate between hydrogen and deuterium of palladium. *J Nucl Mater* 1995;226:311–8.
- [67] Liu Y, Wu W, Zhang G, Fang M, Jing W, Xiong Y, et al. Study of separation factor and product extraction ratio in hydrogen isotope separation with displacement chromatography. *Fusion Eng Des* 2021;165:112246.
- [68] Deng X, Luo D, Qin C, Qian X, Yang W. Hydrogen isotopes separation using frontal displacement chromatography with Pd-Al₂O₃ packed column. *Int J Hydrogen Energy* 2012;37:10774–8.
- [69] Ducret D, Laquerbe C, Ballanger A, Steimetz J, Porri V, Verdin JP, et al. Separation of hydrogen isotopes by thermal cycling absorption process: an experimental device. *Fusion Sci Technol* 2002;41:1092–6.
- [70] Jiang Y, Ji F, Feng Y, Ye X, Ni M. Effect of alumina on thermodynamic performance of palladium-H₂ (D₂) system. *Int J Hydrogen Energy* 2022;47:18088–97.
- [71] Xiao X, Heung LK, Sessions HT. Recent advances in SRS on hydrogen isotope separation using thermal cycling absorption process. *Fusion Sci Technol* 2015;67:643–6.
- [72] Du X, Ye X, Chen Ca, Jiang C. Hydrogen isotope effect of nanoporous palladium. *Int J Hydrogen Energy* 2021;46:1023–9.
- [73] Liu R, Peng Y, Rong W, Cao Q. Thermodynamics and kinetics of hydrogen isotope effects of hydrogen/deuterium absorption in Pd-5wt.%Pt alloy. *Int J Hydrogen Energy* 2023.
- [74] couk Gold. All time palladium price. 2021.
- [75] Lässer R, Bainbridge N, Bell AC, Brennan D, Hemmerich JL, Knipe S, et al. Hydrogen isotope separation in the JET active gas handling system during DTE1. 1998.
- [76] Botter F, Tistchenko S, Hircq B. Separation of hydrogen isotopes by displacement gas chromatography. In: Keen BE, Huguet M, Hemsworth R, editors. *Fusion technology* 1990. Oxford: Elsevier; 1991. p. 713–7.
- [77] Sazonov AB, Magomedbekov EP. Estimate of the efficiency of hydrogen-metal hydride (intermetallic compound) systems in the separation of the three-isotope mixtures H–D–T. *Atom Energy* 2000;89:736–44.
- [78] Kawamura Y, Onishi Y, Okuno K, Yamanishi T. Hydrogen isotope separation capability of low temperature mordenite column for gas chromatograph. *Fusion Eng Des* 2008;83:1384–7.
- [79] Yamanishi T, Kudo H. Adsorption equilibrium of hydrogen isotopes on alumina adsorbents for gas-solid chromatography. *J Chromatogr A* 1989;475:125–34.
- [80] Cai J, Xing Y, Yang M, Zhao X. Preparation of modified γ -alumina as stationary phase in gas-solid chromatography and its separation performance for hydrogen isotopes. *Adsorption* 2013;19.
- [81] Yang S, Xie H, Zhu H, Zhang L, Zhou Y, Zhang H, et al. Highly effective hydrogen isotope separation by cryogenic gas chromatography in a new stationary phase material MnCl₂@CPL-1@ γ -Al₂O₃. *Int J Hydrogen Energy* 2018;43:7973–81.
- [82] Lässer R, Grünhagen S, Kawamura Y. Use of micro gas chromatography in the fuel cycle of fusion reactors. *Fusion Eng Des* 2003;69:813–7.
- [83] Andreev BM, Kruglov AV, Selivanenko YL. Continuous isotope separation in systems with solid phase. I. Gas-phase separation of isotopes of the light elements. *Separ Sci Technol* 1995;30:3211–27.
- [84] Cheh CH, Chew VS, Weng C, Yao Q, Holzhueter IB. Advanced gas chromatographic system testing. *Fusion Technol* 1995;28:561–5.
- [85] Fukada S, Fuchinoue K, Nishikawa M. Hydrogen isotope separation based on isotopic exchange in palladium bed. *Fusion Technol* 1995;28:608–13.
- [86] Fukada S, Yamasaki T, Matsuo H, Mitsuishi N. Experimental and analytical studies on chromatography of hydrogen-deuterium mixtures with vanadium particle fixed-bed. *J Nucl Sci Technol* 1990;27:642–50.
- [87] Wiswall RH, Reilly JJ. Inverse hydrogen isotope effects in some metal hydride systems. *Inorg Chem* 1972;11:1691–6.
- [88] Hill FB, Grzetic V. Cascades for hydrogen isotope separation using metal hydrides. *J Less Common Metals* 1983;89:399–405.

- [89] Golubkov AN, Yukhimchuk AA. Equilibrium pressure of protium and deuterium over vanadium dihydride phase. In: Hampton MD, Schur DV, Zaginaichenko SY, Trefilov VI, editors. Hydrogen materials science and chemistry of metal hydrides. Dordrecht: Springer Netherlands; 2002. p. 255–64.
- [90] Wiswall R, Reilly J, Bloch F, Wirsing E. Hydrogen isotope exchange in metal hydride columns. United States; 1977.
- [91] Fukada S, Fuchinoue K, Nishikawa M. Hydrogen isotope separation using particle beds of LaNi₃Al₂ hydride. *J Alloys Compd* 1993;201:49–55.
- [92] Soga K, Imamura H, Ikeda S. Hydrogen-deuterium equilibration on LaNi₅H_{sub} (35). *Nippon Kagaku Kaishi* 1977;1977:1304–10.
- [93] Reilly JJ. Metal hydride technology. Upton, NY (USA): Brookhaven National Lab.; 1979.
- [94] Andreev BM, Magomedbekov EP. Separation of hydrogen isotopes by chemical isotope exchange in systems involving metal and intermetallic compound hydrides. *Separ Sci Technol* 2001;36:2027–86.
- [95] Kang H-g, Chung D-y, Oh YH, Chang MH, Yun S-H. Experimental comparison on heat transfer-enhancing component of metal hydride bed. *Fusion Eng Des* 2016; 109–111:965–9.
- [96] Fukada S, Yamasaki T, Matsuo H, Mitsuishi N. The rate of an exchange reaction of hydrogen and deuterium in a Mg₂Ni bed. *Int J Hydrogen Energy* 1991;16: 809–13.
- [97] Vogd R, Ringel H, Hackfort H, Schober T, Dieker C. Gas chromatographic separation of hydrogen isotopes on molecular sieves. *Fusion Technol* 1988;14: 574–8.
- [98] Junbo Z, Liping G, Kuisheng W. Hydrogen isotope separation by cryogenic gas chromatography using the combined column of 5Åmolecular sieve and Al₂O₃. *Int J Hydrogen Energy* 2006;31:2131–5.
- [99] Imoto S, Tanabe T, Utsunomiya K. Separation of hydrogen isotopes with uranium hydride. *Int J Hydrogen Energy* 1982;7:597–601.
- [100] Shugard AD, Buffleben GM, Johnson TA, Robinson DB. Isotope exchange between gaseous hydrogen and uranium hydride powder. *J Nucl Mater* 2014;447:304–13.
- [101] Banos A, Harker NJ, Scott TB. A review of uranium corrosion by hydrogen and the formation of uranium hydride. *Corrosion Sci* 2018;136:129–47.
- [102] Lässer R, Jones G, Hemmerich JL, Stagg R, Yorkshades J. The preparative gas chromatographic system for the JET active gas handling system - inactive commissioning. *Fusion Technol* 1995;28:681–6.
- [103] Wicke E. Isotope effects in palladium-hydrogen systems the concentration of deuterium and tritium. *Platinum metals rev* 1971;15:144.
- [104] Reddy B, Mistry K, Kumar R, Mohan S, Mahajani S. Recovery of deuterium from hydrogen-deuterium mixture using palladium. *Separ Sci Technol* 2016;51: 784–96.
- [105] Fukada S, Fujiwara H. Comparison of chromatographic methods for hydrogen isotope separation by Pd beds. *J Chromatogr A* 2000;898:125–31.
- [106] Flanagan TB, Oates WA. The palladium-hydrogen system. *Annu Rev Mater Sci* 1991;21:269–304.
- [107] Sicking G. Isotope effects in metal-hydrogen systems. *J Less Common Metals* 1984;101:169–90.
- [108] Bourgeois N, Crivello J-C, Cenedese P, Paul-Boncour V, Joubert J-M. Vibration analysis of hydrogen, deuterium and tritium in metals: consequences on the isotope effect. *J Phys Condens Matter* 2018;30:335402.
- [109] Anand NS, Pati S, Jat RA, Parida SC, Mukerjee SK. Hydrogen isotope effect on thermodynamic properties of Pd_{0.9}X_{0.1} (X=Cu, Ag and Au) alloys. *Int J Hydrogen Energy* 2017;42:3136–41.
- [110] Luo W, Cowgill DF, Flanagan TB. Separation factors for hydrogen isotopes in palladium hydride. *J Phys Chem C* 2013;117:13861–71.
- [111] Andreev BM, Magomedbekov EP, Sicking G. Interaction of hydrogen isotopes with transition metals and intermetallic compounds. Berlin, Heidelberg: Springer; 1996.
- [112] Luo W, Cowgill D, Causey R, Stewart K. Equilibrium isotope effects in the preparation and isothermal decomposition of ternary hydrides Pd(HxD_{1-x}Y) (0 < x < 1 and y > 0.6). *J Phys Chem B* 2008;112:8099–105.
- [113] Pati S, Jat RA, Anand NS, Derose DJ, Karn KN, Mukerjee SK, et al. Pd-Ag-Cu dense metallic membrane for hydrogen isotope purification and recovery at low pressures. *J Membr Sci* 2017;522:151–8.
- [114] Heung LK, Sessions HT, Xiao X, Mentzer HL. Demonstration of the next-generation TCAP hydrogen isotope separation process. *Fusion Sci Technol* 2009; 56:1471–5.
- [115] Keshaviah VR, Hamrin Jr CE. Parametric pumping and its application to the separation of isotopes Progress report, June 1. United States; 1970–May 31, 1971. p. 108.
- [116] Hamrin Jr CE. Isotope separation by parametric pumping and heatless adsorption. Final report. Kentucky Univ.; 1973.
- [117] Yan Y, Li F, Deng L, Wang M, Tang T, Fang M, et al. A fresh look at thermal cycling absorption process for hydrogen isotopes separation by dynamic simulation: initial feeding process and total reflux mode. *Int J Hydrogen Energy* 2023;48:23894–908.
- [118] Mosley WC. Pd/k for RTF and 232-H TCAP units. United States; 1991.
- [119] Heung LK, Sessions HT, Poore AS, Jacobs WD, Williams CS. Next-generation TCAP hydrogen isotope separation process. *Fusion Sci Technol* 2008;54:399–402.
- [120] Heung LK, Sessions HT, Xiao X. TCAP hydrogen isotope separation using palladium and inverse columns. *Fusion Sci Technol* 2011;60:1331–4.
- [121] Zhou J, Zhang X, Hao S, Huang W. Dynamic simulation of Thermal Cycling Absorption Process with twin columns for hydrogen isotopes separation. *Int J Hydrogen Energy* 2014;39:13873–9.
- [122] Guangda L, Guoqiang J, Cansheng S. An experimental investigation for hydrogen and deuterium separation by thermal cycling absorption process. *Fusion Technol* 1995;28:672–5.
- [123] Fujita H, Okada S, Fujita K, Sakamoto H, Higashi K, Hyodo T. Ratio of permeabilities of tritium to protium through palladium-alloy membrane. *J Nucl Sci Technol* 1980;17:436–42.
- [124] Clark EA, Dauchess DA, Heung LK, Rabun RL, Motyka T. Experience with palladium diffusers in tritium processing. *Fusion Technol* 1995;28:566–72.
- [125] Luo DL, Shen CS, Meng DQ. Hydrogen isotope separation factors on palladium alloy membranes. *Fusion Sci Technol* 2002;41:1142–5.
- [126] Nishikawa M, Shiraishi T, Kawamura Y, Takeishi T. Permeation rate of hydrogen isotopes through palladium-silver alloy. *J Nucl Sci Technol* 1996;33:774–80.
- [127] Evans J, Harris IR, Ross DK. A proposed method of hydrogen isotope separation using palladium alloy membranes. *J Less Common Metals* 1983;89:407–14.
- [128] Guangda L, Guikai Z, Miao C, Xiaoying W. Tritium aging effects on hydrogen permeation through Pd_{8.5}Y_{0.19}Ru alloy membrane. *Fusion Eng Des* 2011;86: 2220–2.
- [129] Al-Mufachi NA, Rees NV, Steinberger-Wilkens R. Hydrogen selective membranes: a review of palladium-based dense metal membranes. *Renew Sustain Energy Rev* 2015;47:540–51.
- [130] Nishikawa M, Shiraishi T, Murakami K. Solubility and separation factor of protium-enrichment binary component system in palladium. *J Nucl Sci Technol* 1996;33:504–10.
- [131] Serra E, Kemali M, Perujo A, Ross DK. Hydrogen and deuterium in Pd-25 pct Ag alloy: permeation, diffusion, solubilization, and surface reaction. *Metall Mater Trans* 1998;29:1023–8.
- [132] Wileman RCJ, Harris IR. The permeability behaviour of protium and deuterium through a Pd-7.5at.%Y membrane. *J Less Common Metals* 1985;109:367–74.
- [133] Aoki K, Ogata Y, Kusakabe K, Morooka S. Applicability of palladium membrane for the separation of protium and deuterium. *Int J Hydrogen Energy* 1998;23: 325–32.
- [134] Tanaka S, Kiyose R. Isotope separation of hydrogen and deuterium by permeation through palladium membrane. *J Nucl Sci Technol* 1979;16:923–5.
- [135] Fuerst TF, Taylor CN, Shimada M, Way JD, Wolden CA. High temperature deuterium enrichment using TiC coated vanadium membranes. *J Vac Sci Technol A* 2019;37:021501.
- [136] Dolan MD, Lamb KE, Evtimova JB, Viano DM. Deuterium enrichment using vanadium membranes. *Int J Hydrogen Energy* 2017;42:24183–8.
- [137] Noh SJ, Lee SK, Kim HS, Yun SH, Joo HG. Deuterium permeation and isotope effects in nickel in an elevated temperature range of 450–850 °C. *Int J Hydrogen Energy* 2014;39:12789–94.
- [138] Sakaguchi H, Yagi Y, Shiokawa J, Adachi G. Hydrogen isotope separation using rare earth alloy films deposited on polymer membranes. *J Less Common Metals* 1989;149:185–91.
- [139] Paglieri SN, Way JD. Innovations in palladium membrane research. *Separ Purif Methods* 2002;31:1–169.
- [140] Løvvik OM, Zhao D, Li Y, Bredesen R, Peters T. Grain boundary segregation in Pd-Cu alloys for high permeability hydrogen separation membranes. *Membranes* 2018;8:81.
- [141] Fort D, Farr JPG, Harris IR. A comparison of palladium-silver and palladium-yttrium alloys as hydrogen separation membranes. *J Less Common Metals* 1975; 39:293–308.
- [142] McCord S. An investigation into the use of coated vanadium alloys for the purpose of hydrogen separation. The University of Sheffield; 2017.
- [143] Fuerst TF, Humrickhouse PW, Taylor CN, Shimada M. Surface effects on deuterium permeation through vanadium membranes. *J Membr Sci* 2021;620: 118949.
- [144] Song G, Dolan MD, Kellam ME, Liang D, Zambelli S. V–Ni–Ti multi-phase alloy membranes for hydrogen purification. *J Alloys Compd* 2011;509:9322–8.
- [145] Gade SK, Chmelka SJ, Parks S, Way JD, Wolden CA. Dense carbide/metal composite membranes for hydrogen separations without platinum group metals. *Adv Mater* 2011;23:3585–9.
- [146] Li F, Zhong B, Xiao H, Ye X, Lu L, Guan W, et al. Effect of degassing treatment on the deuterium permeability of Pd-Nb-Pd composite membranes during deuterium permeation. *Separ Purif Technol* 2018;190:136–42.
- [147] Asano K, Hashimoto Y, Iida T, Kondo M, Iijima Y. Hydrogen diffusion by substitution of aluminum and cobalt for a part of nickel in LaNi₅-H alloy. *J Alloys Compd* 2005;395:201–8.
- [148] Glugla M, Cristescu IR, Cristescu I, Demange D. Hydrogen isotope separation by permeation through palladium membranes. *J Nucl Mater* 2006;355:47–53.
- [149] Luo DL, Xiong YF, Song JF, Huang GQ. Hydrogen isotope separation factor measurement for single stage hydrogen separators and parameters for a large-scale separation system. *Fusion Sci Technol* 2005;48:156–8.
- [150] Suzuki Y, Kimura S. Separation and concentration of hydrogen isotopes by a palladium alloy membrane. *Nucl Technol* 1993;103:93–100.
- [151] Tebus V, Rivkis L, Arutunova G, Dmitrievsky E, Filin V, Golikov Y, et al. Investigation of palladium alloy properties degradation during long-time tritium exposure. *J Nucl Mater* 1999;271–272:345–8.
- [152] Klevtsov VG, Boitsov IE, Vedenev AI, Glagolev MV, Lobanov VN, Malkov IL, et al. The impact of tritium on the structure and properties of Pd-membranes. *Fusion Eng Des* 2000;49–50:873–7.
- [153] Choppin G, Liljenzin J-O, Rydberg J, Ekberg C. 3.8.4 gaseous diffusion. Radiochemistry and nuclear chemistry, Elsevier.
- [154] Tsoufanidis N. 3.4 enrichment of uranium by gaseous diffusion. Nuclear fuel cycle: ANS (American Nuclear Society).

- [155] Bonnett I, Busigin A, Shapiro A. Tritium removal and separation technology developments. *Fusion Sci Technol* 2008;54:209–14.
- [156] Borisevich O, Antunes R, Demange D. Comparison of MFI-ZSM5 and NaA zeolite-type tubular membranes for the separation of water vapour from helium for tritium processes in future fusion reactors. *Fusion Eng Des* 2017;125:134–8.
- [157] Michalkiewicz B, Koren ZC. Zeolite membranes for hydrogen production from natural gas: state of the art. *J Porous Mater* 2015;22:635–46.
- [158] Iwai Y, Hiroki A, Tamada M, Isobe K, Yamanishi T. Radiation deterioration of ion-exchange Nafion N117CS membranes. *Radiat Phys Chem* 2010;79:46–51.
- [159] Lozada-Hidalgo M, Zhang S, Hu S, Esfandiari A, Grigorieva IV, Geim AK. Scalable and efficient separation of hydrogen isotopes using graphene-based electrochemical pumping. *Nat Commun* 2017;8:15215.
- [160] Lozada-Hidalgo M, Hu S, Marshall O, Mishchenko A, Grigorenko AN, Dryfe RAW, et al. Sieving hydrogen isotopes through two-dimensional crystals. *Science* 2016; 351:68.
- [161] Bukola S, Liang Y, Korzeniewski C, Harris J, Creager S. Selective proton/deuteron transport through Nafion/Graphene/Nafion sandwich structures at high current density. *J Am Chem Soc* 2018;140:1743–52.
- [162] An Y, Oliveira AF, Brumme T, Kuc A, Heine T. Stone–wales defects cause high proton permeability and isotope selectivity of single-layer graphene. *Adv Mater* 2020;32:2002442.
- [163] Yasuda S, Matsushima H, Harada K, Tanii R, Terasawa T-o, Yano M, et al. Efficient hydrogen isotope separation by tunneling effect using graphene-based heterogeneous electrocatalysts in electrochemical hydrogen isotope pumping. *ACS Nano* 2022;16:14362–9.
- [164] Yang L, Cong E, Hao Z, Bo C, Cui Y, Xu S, et al. Selective penetration mechanism of hydrogen isotope through graphene membrane. *Carbon* 2022;200:430–6.
- [165] Bartolomei M, Hernández MI, Campos-Martínez J, Hernández-Lamonedaa R, Giorgi G. Permeation of chemisorbed hydrogen through graphene: a flipping mechanism elucidated. *Carbon* 2021;178:718–27.
- [166] Xue X, Chu X, Zhang M, Wei F, Liang C, Liang J, et al. High hydrogen isotope separation efficiency: graphene or catalyst? *ACS Appl Mater Interfaces* 2022;14: 32360–8.
- [167] Shibuya S, Matsushima H, Ueda M. Study of deuterium isotope separation by PEFC. *J Electrochem Soc* 2016;163:F704–7.
- [168] Stojić DL, Miljanić SS, Grozdić TD, Golobočanin DD, Sovili SP, Jakić MM. D/H isotope separation efficiency in water electrolysis. Improvement by in situ activation at different temperatures. *Int J Hydrogen Energy* 1994;19:587–90.
- [169] Ayers KE, Anderson EB, Capuano C, Carter B, Dalton L, Hanlon G, et al. Research advances towards low cost, high efficiency PEM electrolysis. *ECS Trans* 2019;33: 3–15.
- [170] Ito H, Maeda T, Nakano A, Takenaka H. Properties of Nafion membranes under PEM water electrolysis conditions. *Int J Hydrogen Energy* 2011;36:10527–40.
- [171] Urey HC, Brickwedde FG, Murphy GM. A hydrogen isotope of mass 2 and its concentration. *Phys Rev* 1932;40:1–15.
- [172] Rae HK. Selecting heavy water processes. Separation of hydrogen isotopes. AMERICAN CHEMICAL SOCIETY; 1978. p. 1–26.
- [173] Inoue M, Konishi S, Yamanishi T, Ohira S, Watanabe T, Okuno K, et al. Isotope separation system experiments at the TSTA. *Fusion Technol* 1992;21:293–8.
- [174] Sherman RH, Bartlit JR, Gruetzmacher KM, Yoshida H, Yamanishi T, Naito T, et al. Operation of the TSTA isotope separation system with 100 gram tritium. *Fusion Technol* 1988;14:1273–6.
- [175] Anderson JL, Bartlit JR. Tritium technology studies at the tritium systems test assembly. *Fusion Technol* 1986;10:1329–33.
- [176] Lässer R, Bell AC, Bainbridge N, Brennan PD, Grieveson B, Hemmerich JL, et al. Overview of the performance of the JET active gas handling system during and after DTE1. *Fusion Eng Des* 1999;47:173–203.
- [177] Bellamy DG, Robins JR, Woodall KB, Sood SK, Gierszewski P. ITER relevant testing of a cryogenic distillation column system. *Fusion Technol* 1995;28:525–9.
- [178] Radebaugh R. Refrigeration for superconductors. *Proc IEEE* 2004;92:1719–34.
- [179] Agency IAE. ITER technical basis. Vienna. 2002.
- [180] Busigin A, Busigin CJ, Robins JR, Woodall KB, Bellamy DG, Fong C, et al. Installation and early operation of a complex low inventory cryogenic distillation system for the Princeton TFTR. *Fusion Technol* 1995;28:1312–6.
- [181] Robins JR, Woodall KB, Woo G, Bellamy DG, Sood SK, Fong C, et al. Tritium purification system for TFTR. 15th IEEE/NPSS symposium fusion engineering, vol. 1; 1993. p. 69–72.
- [182] Bainbridge N, Bell AC, Brennan PD, Knipe S, Lässer R, Stagg R. Operational experience with the JET AGHS cryodistillation system during and after DTE1. *Fusion Eng Des* 1999;47:321–32.
- [183] Iwai Y, Yamanishi T, Nakamura H, Isobe K, Nishi M, Willms RS. Numerical estimation method of the hydrogen isotope inventory in the hydrogen isotope separation system for fusion reactor. *J Nucl Sci Technol* 2002;39:661–9.
- [184] Bhattacharyya R, Bhanja K, Mohan S. Simulation studies of the characteristics of a cryogenic distillation column for hydrogen isotope separation. *Int J Hydrogen Energy* 2016;41:5003–18.
- [185] Piché S, Larachi F, Grandjean BPA. Improved liquid hold-up correlation for randomly packed towers. *Chem Eng Res Des* 2001;79:71–80.
- [186] Hill AK, Chantler G, Jackson T. Modelling of a three-column hydrogen distillation cascade for DEMO with updated physical property predictions and an assessment of correlations for prediction of liquid holdup. 2021. To be published.
- [187] Yamanishi T, Kinoshita M. Preliminary experimental study for cryogenic distillation column with small inner diameter, (II). *J Nucl Sci Technol* 1984;21: 853–61.
- [188] Yamanishi T, Enoeda M, Okuno K, Hayashi T, Amano J, Naruse Y, et al. Experimental study for separation characteristics of cryogenic distillation columns with an H-D-T system. *Fusion Technol* 1991;20:419–24.
- [189] Alekseev I, Fedorchenko O, Kravtsov P, Vasilyev A, Vnuzdavaev M. Experimental results of hydrogen distillation at the low power cryogenic column for the production of deuterium depleted hydrogen. *Fusion Sci Technol* 2008;54:407–10.
- [190] Stefan I, Balteanu O, Bucur C, Vijulie M, Sofilca N, Moraru C, et al. Overview about cryogenic distillation control and safety approach for Isotopes Separation Facility (ISF). *Fusion Eng Des* 2020;159:111771.
- [191] Ana G, Cristescu I, Draghia M, Bucur C, Balteanu O, Vijulie M, et al. Construction and commissioning of a hydrogen cryogenic distillation system for tritium recovery at ICIT Rm. Valcea. *Fusion Engineering and Design* 2016;106:51–5.
- [192] Bornea A, Zamfirache M, Stefan L, Stefanescu I, Preda A. Experimental investigation on hydrogen cryogenic distillation equipped with package made by ICIT. *Fusion Sci Technol* 2015;67:266–9.
- [193] Bornea A, Zamfirache M, Stefanescu I, Preda A, Balteanu O, Stefan I. Investigation related to hydrogen isotopes separation by cryogenic distillation. *Fusion Sci Technol* 2008;54:426–9.
- [194] Ohta T, Bouchigny S, Didelez JP, Fujiwara M, Fukuda K, Kohri H, et al. Distillation of hydrogen isotopes for polarized HD targets. *Nucl Instrum Methods Phys Res Sect A Accel Spectrom Detect Assoc Equip* 2012;264:347–52.
- [195] Cristescu I, Cristescu IR, Dörr L, Gluga M, Hellriegel G, Kveton O, et al. TRENTA facility for trade-off studies between combined electrolysis catalytic exchange and cryogenic distillation processes. *Fusion Sci Technol* 2005;48:97–101.
- [196] Young JS, Sherman RH, Willms RS, Iwai Y, Nishi M. Steady-state computer modeling of a recent H-D-T cryogenic distillation experiment at TSTA. *Fusion Sci Technol* 2002;41:1131–6.
- [197] Yamanishi T, Okuno K. Mass transfer in cryogenic distillation column separating hydrogen isotopes. *J Nucl Sci Technol* 1994;31:562–71.
- [198] Yamanishi T, Yoshida H, Hirata S, Naito T, Naruse Y, Sherman RH, et al. Single column and two-column H-D-T distillation experiments at TSTA. *Fusion Technol* 1988;14:489–94.
- [199] Enoeda M, Yamanishi T, Yoshida H, Naruse Y, Fukui H, Muta K. Hydrogen isotope separation characteristics of cryogenic distillation column. *Fusion Eng Des* 1989; 10:319–23.
- [200] Yamanishi T, Enoeda M, Yoshida H, Naruse Y, Fukui H, Nagai H, et al. Experimental apparatus for cryogenic hydrogen isotope separation process in the tritium process laboratory. *Fusion Technol* 1988;14:495–500.
- [201] Ana G, Sofilca N, Niculescu A, Draghia M. Investigation of some critical scenarios due to various failures of ICSI Cryogenic Distillation System. *Fusion Eng Des* 2017;124:861–4.
- [202] Ana G, Vladulescu F, Ana R, Pasca G, Niculescu A. Thermal analysis of a cryogenic distillation column for hydrogen isotopes separation. *Fusion Eng Des* 2019;146: 1868–71.
- [203] Lefebvre X, Hollingsworth A, Parracho A, Dalgliesh P, Butler B, Smith R. Conceptual design and optimization for jet water detritiation system cryo-distillation facility. *Fusion Sci Technol* 2015;67:451–4.
- [204] Kinoshita M, Matsuda Y, Naruse Y, Tanaka K. Computer analysis on steady state separation characteristics of hydrogen isotope separation system by cryogenic distillation. *J Nucl Sci Technol* 1981;18:525–39.
- [205] Buvat JC, Latge C, Joulia X, Pautrot GP. Simulation of hydrogen isotope separation by cryogenic distillation. *Fusion Technol* 1992;21:954–9.
- [206] Niculescu A, Constantin T, Ana G, Draghia M. Dynamic simulation of a multicomponent distillation column for D-T separation. *Fusion Eng Des* 2017;124: 752–6.
- [207] Busigin A, Sood SK. Steady state and dynamic simulation of the ITER hydrogen isotope separation system. *Fusion Technol* 1995;28:544–9.
- [208] Chen M, Li P, Hu C, Luo J, Wen M, Yu B, et al. Dynamic simulation of a cryogenic batch distillation process for hydrogen isotopes separation. *Int J Hydrogen Energy* 2022;47:11955–61.
- [209] Koo IG, Lee WM. Hydrogen isotope separation by plasma-chemical method. *J Nucl Sci Technol* 2005;42:717–23.
- [210] Ovcharov AV. More precise values of separation factors in water-hydrogen isotopic exchange for modeling of combined electrolysis and catalytic exchange process. *Fusion Sci Technol* 2017;71:333–8.
- [211] Yamamoto I, Inoue A, Kanagawa A. Measurement of separative characteristics of H2-HT isotope separation using thermal diffusion column. *J Nucl Sci Technol* 1988;25:704–11.
- [212] Müller G, Vasaru G. The clausius-dickel thermal diffusion column – 50 Years after its invention. *Isotopenpraxis Isotopes in Environmental and Health Studies* 1988; 24:455–64.
- [213] Yamakawa H, Matsumoto K, Enokida Y, Yamamoto I. Effect of operational pressure on periodic oscillation of secondary circulation near the bottom of the thermal diffusion column. *J Nucl Sci Technol* 1999;36:297–303.
- [214] Ho CD, Su YC, Guo JJ, Chen SH. Theoretical and experimental studies on the heavy water enrichment by thermal diffusion for improved performance under countercurrent-flow frazier scheme and flow-rate fraction variations. *Separ Sci Technol* 2005;39:2299–322.
- [215] Ho C-D, Yeh H-M, Hsu C-C. Recovery of deuterium from H–D gas mixture in thermal diffusion columns connected in series with countercurrent-flow transverse sampling streams. *Int J Hydrogen Energy* 2016;41:10819–26.
- [216] Yeh H-M, Hsu C-C. Separation of deuterium from H–D gas mixture by thermal diffusion in the devices of multi concentric-tube columns with total sum of column heights fixed. *J Nucl Mater* 2010;406:317–22.

- [217] Yamamoto I, Kanagawa A. Possibility of remarkable enhancement of separation factor by “cryogenic-wall” thermal diffusion column. *J Nucl Sci Technol* 1990;27:250–5.
- [218] Yamakawa H, Matsumoto K, Enokida Y, Yamamoto I. Numerical analysis of dynamic behavior at start-up of the thermal diffusion column for hydrogen isotope separation. *J Nucl Sci Technol* 1999;36:198–203.
- [219] Ortman MS, Heung LK, Nobile A. III RLR. Tritium processing at the Savannah River Site: present and future. *J Vac Sci Technol A* 1990;8:2881–9.
- [220] Mitsui J, Okada Y, Sakai F, Ide T, Hirata K, Yamanishi T, et al. Separation of hydrogen isotopes by an advanced thermal diffusion column using cryogenic-wall. *Fusion Technol* 1991;19:1646–50.
- [221] Gummer J, Hawksworth S. Spontaneous ignition of hydrogen literature review Health and Safety Executive 2008. Health and Safety Laboratory Health and Safety Executive; 2008.
- [222] Letokhov VS. Laser-induced chemistry — basic nonlinear processes and applications. In: Medin H, Swanberg S, editors. *Laser technology in chemistry*. Berlin, Heidelberg: Springer Berlin Heidelberg; 1988. p. 237–51.
- [223] Letokhov VS, Moore CB. Laser isotope separation. *Sov J Quant Electron* 1976;6:129–50. submitted for publication.
- [224] Paisner JA. Atomic vapor laser isotope separation. In: Medin H, Swanberg S, editors. *Laser technology in chemistry*. Berlin, Heidelberg: Springer Berlin Heidelberg; 1988. p. 253–60.
- [225] Makide Y, Kato S, Tominaga T, Takeuchi K. Laser isotope separation of tritium from deuterium: CO₂-laser-induced multiphoton dissociation of C₂Tf₅ in C₂Df₅. *Appl Phys B* 1983;32:33–4.
- [226] Nayak A, Sarkar S, Biswas D, RamaRao K, Mittal J. Separation of tritium from deuterium by pulsed NH₃ laser-selective multiple photon dissociation of CTCl₃. *Appl Phys B* 1991;53:246–9.
- [227] Magnotta F, Herman IP, Aldridge FT. Highly selective tritium-from-deuterium isotope separation by pulsed NH₃ laser multiple-photon dissociation of chloroform. *Chem Phys Lett* 1982;92:600–5.
- [228] Evans DK, McAlpine RD, Adams HM. The multiphoton absorption and decomposition of fluoroform-d: laser isotope separation of deuterium. *J Chem Phys* 1982;77:3551–8.
- [229] Freund S, Maier W, Beattie W, Holland R. Laser-induced separation of hydrogen isotopes in the liquid phase. United States: US Department of Energy; 1977.
- [230] Yeung ES, Moore CB. Isotopic separation by photopredissociation. *Appl Phys Lett* 1972;21:109–10.
- [231] Mannik L, Brown SK. Deuterium separation by ultraviolet laser dissociation of formaldehyde. *J Appl Phys* 1982;53:6620–7.
- [232] Hsu D, Manuccia T. Separation of hydrogen isotopes. United States: US Secretary of Navy; 1983.
- [233] Mayer SW, Kwok MA, Gross RWF, Spencer DJ. Isotope separation with the cw hydrogen fluoride laser. *Appl Phys Lett* 1970;17:516–9.